# TECHNICAL REPORT R-43

## ANALYSIS OF INJECTION-VELOCITY EFFECTS ON ROCKET MOTOR DYNAMICS AND STABILITY

By HERBERT G. HURRELL

Lewis Research Center
Cleveland, Ohio

# TECHNICAL REPORT R-43

## ANALYSIS OF INJECTION-VELOCITY EFFECTS ON ROCKET MOTOR DYNAMICS AND STABILITY

By HERBERT G. HURRELL


### SUMMARY

*Combustion time lag is treated in a form that includes its dependency on injection velocity, such dependency being indicated by recent studies. This generalized form is used in analyses of low-frequency chamber dynamics and combustion instability (tank-fed rocket). The theoretical responses and stability boundaries obtained are compared with those given with the previous time-lag concept. It is concluded that the injection-velocity effect on the time lag cannot be neglected in the theory of chamber dynamics and combustion instability.*


### INTRODUCTION

In the field of liquid-propellant rocket engines, there is widespread interest in the theory of combustion-chamber dynamics. In the past, this interest was generated primarily by the frequent occurrence of combustion instability. Often costly and time-consuming development programs were required for new designs in order to overcome this destructive phenomenon. At the present time, although combustion instability is still of much concern, increasing attention is being given to defining the chamber dynamics for control purposes. This late emphasis on controls results from the stringent trajectory requirements of space missions.

The foundation of existing theory was laid in 1941 when Von Kármán recognized that a time lag between propellant injection and combustion was instrumental in combustion instability (ref. 1). This combustion time lag (also known as dead time) was first treated as being of constant duration. It was used in this manner in analyses by Gunder and Friant (ref. 2), Yachter and Waldinger (ref. 3), Summerfield (ref. 4), and Lee, Gore, and Ross (ref. 5). Crocco (refs. 6 and 7) improved the concept by considering the time lag to be a variable with a duration dependent on changing conditions along the path of the propellant in the chamber. For simplicity he correlated the various conditions to chamber pressure. Crocco's time-lag concept was used in stability studies by Tsien (ref. 8) and Marble and Cox (ref. 9). At the present time, Crocco, Grey, and Matthews (ref. 10) are using this concept of pressure-dependency to determine time lags from experimental frequency response. This same concept is the basis of the extensive theory of combustion instability developed by Crocco and Cheng (ref. 11).

Recent developments, however, indicate the time lag must be treated as a function of injection velocity as well as conditions after injection. Studies have shown that the atomization of the propellant is sensitive to injection velocity (refs. 12 and 13). Propellant atomization, in turn, has long been considered an important factor in determining the duration of the time lag (ref. 11, e.g.). Substantiation of this belief is given by the correlation of engine performance with vaporization in reference 14, which indicates that the atomization-sensitive vaporization process may determine the time lag. Experimental evidence that directly shows the variation of time lag with injection velocity is reported by Penner and Fuhs (ref. 15).

The time-lag concept, therefore, is generalized in the present treatment to include the effect of injection velocity. This is done by treating the time lag as being dependent on initial propellant atomization as well as conditions encountered by the propellant in the chamber; the initial atomi-

zation is considered to be a function of injection velocity. The chamber variables along the path of the propellant after injection are correlated, in the manner of Crocco, to chamber pressure.

Analyses are presented that show the importance of using the more general time-lag concept in the treatment of chamber dynamics and combustion instability. With the generalized concept, a small-perturbation equation of the combustion chamber is derived for a bipropellant rocket. The equation treats the range of low frequencies involved in the combustion instability called chugging. This is also the frequency range of primary interest in controls work. From the chamber equation, the transfer functions are formulated, and the frequency response is presented for possible sensitivities of the time lag to injection velocity. The chamber equation is then used in analyzing the stability of a tank-fed rocket in order to illustrate the injection-velocity role in combustion instability.

## SYMBOLS

$B$ mass-transfer number
$D$ drop diameter
$E$ initial or final level of time-lag processes
$F,f$ rate of time-lag processes
$h$ injection-hole diameter, in.
$K$ $\overline{p}/2(P_{o,f}-\overline{p})$
$M$ mass of burnt gas in combustion chamber
$m$ exponent in $F\sim D^m p^n$
$n$ exponent in $F\sim D^m p^n$ (interaction index)
$P_{o,f}$ tank pressure of oxidizer or fuel
$p$ pressure of gas in combustion chamber
$Q$ injection-velocity sensitivity,

$$\begin{cases} \text{zero (eq. (20))} \\ (r+1)(3-m)y\alpha \text{ (eq. (21))} \\ (3-m)y\alpha \text{ (eqs. ((22) and (25))} \end{cases}$$

$R$ gas constant
$Re$ Reynolds number
$r$ mixture ratio, $w_o/w_f$
$Sc$ Schmidt number
$s$ dimensionless complex operator
$T$ gas temperature
$t$ time
$U$ drop velocity relative to gas in chamber
$V$ injection velocity
$w_b$ gas generation rate
$w_e$ exhaust rate
$w_f$ fuel rate
$w_i$ total injection rate
$w_o$ oxidizer rate
$y$ $1\Big/\left\{1-\left[\dfrac{\overline{D}(t)}{\overline{D}(t-\overline{\sigma})}\right]^{3-m}\right\}$ or $1\Big/\left\{1-\left[\dfrac{\overline{D}(z)}{\overline{D}(z-\overline{\tau})}\right]^{3-m}\right\}$
$z$ dimensionless time, $t/\theta_g$
$\alpha$ atomization index ($D\sim V^{-\alpha}$)
$\beta$ dimensionless frequency of neutral oscillation, $\theta_g\omega$, where $\omega$ is angular frequency
$\Delta(\ )$ small perturbations
$\theta_g$ gas residence time
$\mu$ gas viscosity
$\rho_l$ liquid density
$\sigma$ time lag (dead time)
$\tau$ dimensionless time lag, $\sigma/\theta_g$

Superscript:

$(\overline{\ })$ steady-state values

## COMBUSTION-CHAMBER DYNAMICS

### THE TIME LAG

The combustion in a liquid-propellant rocket engine is very complicated and still not fully understood. Intricate processes such as atomization, mixing, vaporization, and chemical reaction take place before the final products of combustion evolve from the injected liquids. Although the evolution is certainly gradual in both time and space, a treatment of the phenomenon in its gradual nature is not warranted by the present knowledge of the processes involved and of the chamber conditions affecting these processes. A working model is obtained, therefore, in the manner of previous authors by considering small fractions of the final products to be generated in a discontinuous manner. That is, the gradual evolution of small elements of propellants into a particle of burnt gas is replaced by a sudden conversion. The time interval between injection and the sudden conversion is called time lag. In general, different particles of burnt gas will have different time lags, and the time lag of each will be a time-dependent quantity. Nevertheless, considerable simplification is achieved in that the complicated combustion process is represented merely by a distribution of gas sources.

It has been shown (ref. 11) that the rate at which the burnt gas is generated from these sources is dependent on the rate of change of the

associated time lags. It is necessary, therefore, to consider the manner in which the time lag varies before proceeding with the analysis of the chamber dynamics.

Previous authors have assumed that the variations in the time lag are caused only by variations in the physical factors encountered by the propellant after injection into the chamber. The assumption is tacitly contained in the equation

$$\int_{t-\sigma}^{t} f(t')\mathrm{d}t' = E(t) = \text{const.} \qquad (1)$$

used to define the dependency of the time lag $\sigma$ on the physical factors. The integral, which is taken over the path of the propellant element from the time of injection $t'=t-\sigma$ to the time of burning $t'=t$, represents the accumulation during the time lag of the processes determining its duration. The process rate $f(t')$ is influenced by the chamber variables such as pressure, temperature, and relative velocities between propellant and gas. The constant right-hand member $E(t)$ represents the final level of the processes, that is, the level to which they must accumulate before the sudden conversion into burnt gas. The equation, of course, is sufficient only with the assumption that the initial level is constant, the general form being

$$E(t-\sigma)+\int_{t-\sigma}^{t} f(t')\mathrm{d}t' = E(t) = \text{const.} \qquad (2)$$

where the term $E(t-\sigma)$ represents the level of the processes, or the condition of the propellant, at the instant of injection.

In the following analysis, this assumption is dropped, and the condition of the propellant at the instant of injection is treated as a variable with an effect on the duration of the time lag. To do this quantitatively, of course, requires that the initial (and final) condition in equation (2) be defined explicitly.

The more explicit equation is obtained in the following manner. The liquid drop is treated as the elemental unit of propellant, and it is postulated that its actual combustion can be adequately depicted by a time-lag approximation controlled by the lifetime of the drop, or a portion thereof. In other words, the sudden conversion to burnt gas, the end of the time lag, is considered to occur when the drop has been reduced to a definite size. (For bipropellants, the species to be treated is the one having longer drop lifetimes.) The rate at which the drop size is reduced at each instant along its path can be expressed by the proportionality

$$\frac{\mathrm{d}D^3}{\mathrm{d}t'} \sim D^m F \qquad (m<3)$$

where $F$ represents a function dependent on chamber variables. The relation can also be written as

$$\frac{\mathrm{d}D^{3-m}}{\mathrm{d}t'} = f \qquad (3)$$

with the proportionality constant being absorbed in the new function $f$. By specifying the size of the drop at the end of the time lag as $D(t)$, the duration of the time lag is defined from equation (3) as follows:

$$\int_{D^{3-m}(t-\sigma)}^{D^{3-m}(t)} \mathrm{d}D^{3-m} = \int_{t-\sigma}^{t} f(t')\mathrm{d}t' \qquad (4)$$

which, upon integration of the left-hand member, becomes

$$D^{3-m}(t-\sigma)+\int_{t-\sigma}^{t} f(t')\mathrm{d}t' = D^{3-m}(t) \qquad (5)$$

It should be noted that the treatment resulting in equation (5) does not necessarily imply the actual combustion process to be one of "drop-burning," in which the vapors issuing from the drop are immediately burned. The model suffices, rather, if the vapors formed along the path of the drop accumulate and burn at a later time; the only condition being, as previously stated, that the actual combustion can be adequately approximated by a discontinuous transformation taken at a definite drop size. The model may not be sufficiently general, of course, for some applications. More generality would be obtained by treating the time lag as the sum of the drop lifetime and a gas-phase delay, each with its own process rate. For high-frequency applications, in which even small delays are significant, the more general treatment appears essential. In fact, the recent work of Crocco, Grey, and Harrje (ref. 16) shows conclusively that small delays highly dependent on chamber pressure are instrumental in high-frequency combustion instability (screaming). Such delays are probably in the gas phase.

For low-frequency applications, such as those in the later sections of the present report, the general formulation may be required if there is considerable combustion delay after the drop vanishes. It is not deemed appropriate, however, to complicate the present work by this generalization since interest is presumed to be centered primarily in rockets with good liquid phase mixing.

In proceeding, therefore, the rate of change of time lag is found from equation (5) to be

$$\frac{d\sigma}{dt}=-\frac{1}{f(t-\sigma)}\frac{dD^{3-m}}{dt}(t-\sigma)-\frac{f(t)-f(t-\sigma)}{f(t-\sigma)} \quad (6)$$

which, for the small-perturbation treatment, can be written as

$$\frac{d\sigma}{dt}=-\frac{1}{\bar{f}(t-\bar{\sigma})}\frac{dD^{3-m}}{dt}(t-\bar{\sigma}) -\frac{\Delta f(t)-\Delta f(t-\bar{\sigma})}{\bar{f}(t-\bar{\sigma})}-\frac{\bar{f}(t)-\bar{f}(t-\bar{\sigma})}{\bar{f}(t-\bar{\sigma})} \quad (7)$$

The process rate $f$ can be expressed, in the manner of Crocco, as

$$f\sim p^n$$

where $n$, the interaction index, includes the effects of other chamber variables under the assumption they can be correlated to pressure. The rate perturbation, therefore, is related to the pressure perturbation by

$$\frac{\Delta f}{\bar{f}}=n\frac{\Delta p}{\bar{p}}$$

and, with uniform pressure in steady-state, equation (7) becomes

$$\frac{d\sigma}{dt}=-\frac{1}{\bar{f}}\frac{dD^{3-m}}{dt}(t-\bar{\sigma})-n\frac{\Delta p(t)-\Delta p(t-\bar{\sigma})}{\bar{p}} \quad (8)$$

An expression for the rate $\bar{f}$ can be obtained by integrating equation (5) for steady-state conditions; substitution into equation (8) yields

$$\frac{d\sigma}{dt}=\frac{\bar{\sigma}}{\bar{D}^{3-m}(t-\bar{\sigma})-\bar{D}^{3-m}(t)}\frac{dD^{3-m}}{dt}(t-\bar{\sigma}) -n\frac{\Delta p(t)-\Delta p(t-\bar{\sigma})}{\bar{p}} \quad (9)$$

The dependence of initial drop size on injection velocity indicated by references 12 and 13 can be expressed for the small perturbation treatment as

$$D(t-\sigma)\sim V^{-\alpha}(t-\sigma)$$

Using this expression with equation (9) gives the following equation relating the rate of change of time lag to perturbations in injection velocity and chamber pressure:

$$\frac{d\sigma}{dt}=-(3-m)y\alpha\bar{\sigma}\frac{d}{dt}\frac{\Delta V}{\bar{V}}(t-\bar{\sigma})-n\left[\frac{\Delta p}{\bar{p}}(t) -\frac{\Delta p}{\bar{p}}(t-\bar{\sigma})\right] \quad (10)$$

where

$$y\equiv\frac{1}{1-\left[\frac{\bar{D}(t)}{\bar{D}(t-\bar{\sigma})}\right]^{3-m}}$$

It should be noted that the pressure perturbation $\Delta p(t)$ appearing in this equation is a function of time and position in general. The position dependence, however, is negligible for frequencies that are low in comparison with the characteristic frequencies of wave propagation in the chamber. As previously stated, these low frequencies are the only ones considered in the later sections of the report.

In general, a precise analytical evaluation of the constants in equation (10) does not appear possible at the present time; the knowledge available concerning the atomization and combustion processes is too limited. Some insight, however, regarding approximate values can be gained for particular cases. For vaporization-limited combustion, Spalding's (ref. 17) modification of the Frössling evaporation equation (ref. 18) offers approximate values of $m$ and $n$. The modified equation can be written as

$$\frac{dD^3}{dt}=\frac{12}{\rho_l}\mu\frac{\ln(1+B)}{Sc}D(1+0.276\ Sc^{1/3}Re^{1/2})$$

from which the exponents for the relation

$$\frac{dD^3}{dt'}\sim D^m p^n$$

are found to be

$$m=\frac{1+\frac{3}{2}0.276\ Sc^{1/3}Re^{1/2}}{1+0.276\ Sc^{1/3}Re^{1/2}}$$

$$n=\frac{1}{2}\left(\frac{0.276\ Sc^{1/3}Re^{1/2}}{1+0.276\ Sc^{1/3}Re^{1/2}}\right)\left(1+\frac{\Delta U/\bar{U}}{\Delta p/\bar{p}}-\frac{\Delta T/\bar{T}}{\Delta p/\bar{p}}\right)$$

when the gas viscosity $\mu$, the transfer number $B$, and the Schmidt number $Sc$ are treated as constants. Since the Schmidt number will be of the order of 0.7, it can readily be seen from the expression for the exponent $m$ that its value will be about 3/2 for high Reynolds number ($Re \gg 16$). Under like circumstances, the interaction index $n$ will have a value near ½ provided the perturbations in relative drop velocity and gas temperature (or their net effect) are small in comparison to the perturbation in pressure. The evaporation equation, of course, must be treated in more detail to obtain an approximate value of the steady-state time lag $\bar{\sigma}$. The more detailed approach was used in calculating the droplet histories presented in reference 19. These histories, which are given for several propellant combinations, offer a convenient means of estimating the steady-state time lag. If the time lag is assumed to include most of the drop lifetime, the quantity $y$ appearing in equation (10) will have a value near unity.

The empirical equation of reference 13 for the mean drop diameter produced by two impinging jets can be used in evaluating the parameter $\alpha$ for injectors of this type. With the assumption of very low gas velocity in the region of impingement, the equation to use is

$$h/D = 2.64\sqrt{h\bar{V}} + 0.97\, h\bar{V}$$

where hole diameter $h$ and drop diameter $D$ are expressed in inches and injection velocity $V$ is in feet per second. From this equation, the formula for $\alpha$ is found to be

$$\alpha = \frac{0.97\, h\bar{V} + 1.32\sqrt{h\bar{V}}}{0.97\, h\bar{V} + 2.64\sqrt{h\bar{V}}}$$

Accordingly, the parameter $\alpha$, which is termed the atomization index, will have values between ½ and unity, depending on the magnitude of the product $h\bar{V}$. For the usual range of $h\bar{V}$ (½ to 7), the formula indicates the atomization index will average about ⅔. This is quickly ascertained from the plot of the formula in figure 1.

If the atomization index $\alpha$ is put equal to zero, the term containing the perturbation in injection velocity disappears from equation (10), and the equation is reduced to the one used by previous authors. Such a procedure, of course, is tantamount to assuming initial drop size to be independent of injection velocity. In view of the observations of references 12, 13, and 15, however, this is not a generally valid assumption, and the complete equation must be used to define the rate of change of the time lag. It is the intent of the following analyses to show the important role the injection-velocity term has in the theory of chamber dynamics and combustion instability. In order to emphasize the relative effect of neglecting this term, the analyses will be made with several simplifying stipulations.

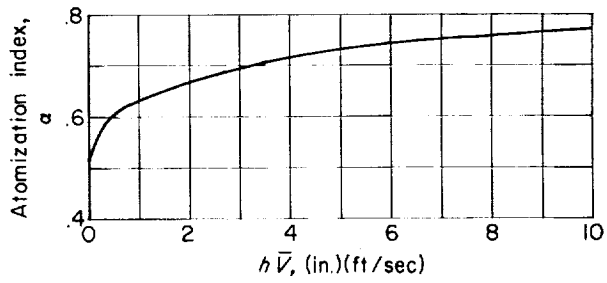


FIGURE 1. Variation of atomization index $\alpha$ with product $h\bar{V}$ of hole diameter and injection velocity for two impinging jets (based on empirical equation of ref. 13).

## CHAMBER EQUATION AND TRANSFER FUNCTIONS

As brought out in the foregoing section, the time-lag concept provides a convenient combustion model consisting of a distribution of burnt-gas sources. As a consequence, the problem of chamber dynamics becomes one of a gas-flow system fed by these sources and depleted by the flow through the nozzle. In accordance with the principle of mass continuity, the excess of the feeding rate over the depletion rate must at each instant be equal to the rate of change of the mass within. In terms of small fractional perturbations, this can be expressed as follows:

$$\frac{\Delta w_b}{\bar{w}_b}(z) - \frac{\Delta w_e}{\bar{w}_e}(z) = \frac{\mathrm{d}}{\mathrm{d}z}\frac{\Delta M}{\bar{M}}(z) \qquad (11)$$

where the dimensionless time $z$ is the ratio of the actual time to the average steady-state residence time of the gas in the chamber. This gas residence time $\theta_g$, of course, is equivalent to $\bar{M}/\bar{w}_i$ and can be evaluated by multiplying the chamber volume by the factor $\bar{p}/\bar{w}_i\bar{R}\bar{T}$.

The perturbation $\Delta w_b/\bar{w}_b$ in the feeding, or gas generation, rate represents the integrated effect of all the sources; the contribution of each source is dependent on the rate of change of its

associated time lag. The general problem involving nonuniform time lags is rather involved algebraically, but can be treated by using the methods of reference 11. For the present purpose, however, the time lag is assumed to be the same for all the sources. With this simplification, the perturbation in the total rate of gas generation can be related to the time lag in the following manner (ref. 11):

$$\frac{\Delta w_b}{\overline{w}_b}(z)=\frac{\Delta w_i}{\overline{w}_i}(z-\overline{\tau})-\frac{\mathrm{d}\tau}{\mathrm{d}z} \tag{12}$$

where the time lag is expressed in the dimensionless form $\tau$, which is equivalent to $\sigma/\theta_g$. By using equation (10) and considering a bipropellant rocket in which the fuel drops have the longer lifetimes, the rate of change of the time lag is given by the equation

$$\frac{\mathrm{d}\tau}{\mathrm{d}z}=-(3-m)y\alpha\overline{\tau}\frac{\mathrm{d}}{\mathrm{d}z}\frac{\Delta w_f}{\overline{w}_f}(z-\overline{\tau}) -n\left[\frac{\Delta p}{\overline{p}}(z)-\frac{\Delta p}{\overline{p}}(z-\overline{\tau})\right] \tag{13}$$

where, at each instant, the pressure is considered uniform throughout the chamber for the range of low frequencies being considered. The fractional change in the total injection rate can be separated into its oxidizer and fuel components by the relation

$$\frac{\Delta w_i}{\overline{w}_i}(z-\overline{\tau})=\frac{r}{r+1}\frac{\Delta w_o}{\overline{w}_o}(z-\overline{\tau})+\frac{1}{r+1}\frac{\Delta w_f}{\overline{w}_f}(z-\overline{\tau}) \tag{14}$$

Upon combining equations (12), (13), and (14), the equation for the perturbation in the rate of burnt-gas generation is found to be

$$\frac{\Delta w_b}{\overline{w}_b}(z)=\frac{r}{r+1}\frac{\Delta w_o}{\overline{w}_o}(z-\overline{\tau})+\frac{1}{r+1}\frac{\Delta w_f}{\overline{w}_f}(z-\overline{\tau}) +(3-m)y\alpha\overline{\tau}\frac{\mathrm{d}}{\mathrm{d}z}\frac{\Delta w_f}{\overline{w}_f}(z-\overline{\tau}) +n\left[\frac{\Delta p}{\overline{p}}(z)-\frac{\Delta p}{\overline{p}}(z-\overline{\tau})\right] \tag{15}$$

In keeping with the intent of the present analysis, the flow leaving the combustion chamber is treated in the following simplified manner. First, it is assumed that the entropy perturbation at the nozzle entrance is negligible. This assumption can be made with reasonable confidence for many applications where the adiabatic flame temperature varies only slightly with mixture ratio in steady state. With this assumption, the dynamics of the unsteady nozzle flow can be accounted for in the low-frequency range simply by including a portion of the nozzle volume in the evaluation of the gas residence time (ref. 20). The nozzle flow, therefore, is treated as if it were steady. Finally, the specific-heat ratio is considered to be unity. Accordingly, the perturbation in the flow of burnt gas from the combustion chamber is given by the equation

$$\frac{\Delta w_e}{\overline{w}_e}(z)=\frac{\Delta p}{\overline{p}}(z) \tag{16}$$

For a more detailed treatment of the exhaust problem, the reader is referred to the work of Cheng (ref. 20), Tsien (ref. 21), and Crocco (ref. 22). (Crocco's treatment is also presented as an appendix in ref. 11.)

The simplification made in regard to the mass-perturbation term of the continuity statement is as follows. It is assumed that at each instant the integral over the chamber length of the entropy perturbation is nearly zero and can be neglected. The perturbation in the total mass of gas within the combustion chamber can be obtained, therefore, from the equation

$$\frac{\Delta M}{\overline{M}}(z)=\frac{\Delta p}{\overline{p}}(z) \tag{17}$$

where the specific-heat ratio is again considered to be unity. A treatment retaining the integrated entropy change is not overly complicated if it is first assumed that the combustion is concentrated in a front near the injector face (ref. 11). Such a treatment, however, exaggerates the entropy effect if the actual combustion is spread at all in the axial direction.

Upon combining equations (15), (16), and (17) with the continuity expression of equation (11), the combustion-chamber equation relating perturbations in pressure and propellant flow is found to be

$$\frac{\mathrm{d}}{\mathrm{d}z}\frac{\Delta p}{\overline{p}}(z)+(1-n)\frac{\Delta p}{\overline{p}}(z)+n\frac{\Delta p}{\overline{p}}(z-\overline{\tau})=-\frac{r}{r+1}\frac{\Delta w_o}{\overline{w}_o}(z-\overline{\tau}) +\frac{1}{r+1}\frac{\Delta w_f}{\overline{w}_f}(z-\overline{\tau})+(3-m)y\alpha\overline{\tau}\frac{\mathrm{d}}{\mathrm{d}z}\frac{\Delta w_f}{\overline{w}_f}(z-\overline{\tau}) \tag{18}$$

Since the solutions of equation (18) are of the type $e^{sz}$, the equation may also be written in operator form as

$$[1+s-n(1-e^{-\bar{\tau}s})]\frac{\Delta p}{\bar{p}}=\frac{r}{r+1}\frac{\Delta w_o}{\bar{w}_o}e^{-\bar{\tau}s}+\frac{1}{r+1}[1+(r+1)(3-m)y\alpha\bar{\tau}s]\frac{\Delta w_f}{\bar{w}_f}e^{-\bar{\tau}s} \quad (19)$$

where the dimensionless operator $s$ is, in general, complex. The factor rendering the operator dimensionless is, of course, the gas residence time.

From equation (19), the following transfer functions of the combustion chamber can be written:

$$\left(\frac{\Delta p/\bar{p}}{\Delta w_o/\bar{w}_o}\right)_{\text{const. } w_f}=\frac{r}{r+1}e^{-\bar{\tau}s}\frac{1}{1+s-n(1-e^{-\bar{\tau}s})} \quad (20)$$

$$\left(\frac{\Delta p/\bar{p}}{\Delta w_f/\bar{w}_f}\right)_{\text{const. } w_o}=\frac{1}{r+1}e^{-\bar{\tau}s}\frac{1+(r+1)(3-m)y\alpha\bar{\tau}s}{1+s-n(1-e^{-\bar{\tau}s})} \quad (21)$$

$$\left(\frac{\Delta p/\bar{p}}{\Delta w_o/\bar{w}_o}\right)_{\text{const. } r}=\left(\frac{\Delta p/\bar{p}}{\Delta w_f/\bar{w}_f}\right)_{\text{const. } r}=e^{-\bar{\tau}s}\frac{1+(3-m)y\alpha\bar{\tau}s}{1+s-n(1-e^{-\bar{\tau}s})} \quad (22)$$

Despite the simplifying assumptions used in the derivation, it is believed these transfer functions describe the predominant form of response for many applications and thus are useful approximations for controls work. It should be remembered, however, that in the present report the fuel drops are considered to have lifetimes longer than those of the oxidizer drops. If the situation is reversed, equations (20) and (21) must be revised as follows:

$$\left(\frac{\Delta p/\bar{p}}{\Delta w_o/\bar{w}_o}\right)_{\text{const. } w_f}=\frac{r}{r+1}e^{-\bar{\tau}s}\frac{1+\frac{r+1}{r}(3-m)y\alpha\bar{\tau}s}{1+s-n(1-e^{-\bar{\tau}s})}$$

$$\left(\frac{\Delta p/\bar{p}}{\Delta w_f/\bar{w}_f}\right)_{\text{const. } w_o}=\frac{1}{r+1}e^{-\bar{\tau}s}\frac{1}{1+s-n(1-e^{-\bar{\tau}s})}$$

In the controls field, it is often convenient to consider dynamic relations in block diagram form; hence, a block diagram representation of the chamber dynamics is given in figure 2. Equation (19) is portrayed by the portion of the diagram drawn in solid lines. The term

$$1+s-n(1-e^{-\bar{\tau}s})$$

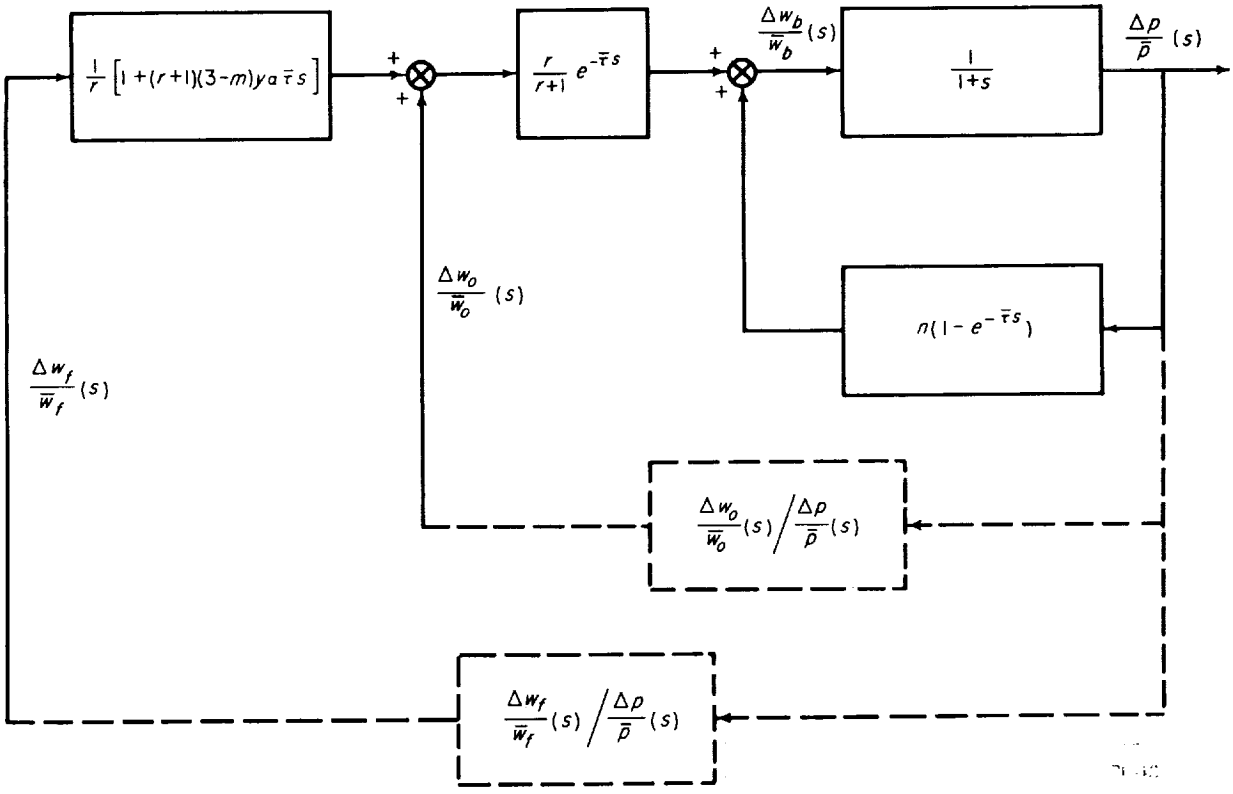


FIGURE 2.—Block diagram of chamber equation (propellant system feedback shown as dashed lines).

of the equation is broken down into an equivalent closed loop in order to emphasize the positive feedback that exists within the combustion chamber. This feedback action, of course, results from the sensitivity of the time lag to chamber pressure. Instability of this internal loop with constant injection rate is treated extensively in reference 11 under the designation "intrinsic instability." In practice, of course, low-frequency combustion instability (chugging) also involves the feedback paths provided by the fuel and oxidizer systems. These external feedbacks, which are negative by virtue of the transfer functions involved, are indicated by the dashed lines in the diagram.

### FREQUENCY RESPONSE

When the chamber transfer functions (eqs. (20), (21), and (22)) are normalized to unity gain, they can be considered in the general form

$$e^{-\bar{\tau}s}\,\frac{1+Q\bar{\tau}s}{1+s-n\,(1-e^{-\bar{\tau}s})}$$

where the parameter $Q$ is defined according to the following table:

| Normalized transfer function | $Q$ |
|---|---|
| $\frac{r+1}{r}\left(\frac{\Delta p/\overline{p}}{\Delta w_o/\overline{w}_o}\right)_{\text{const. } w_f}$ | 0 |
| $(r+1)\left(\frac{\Delta p/\overline{p}}{\Delta w_f/\overline{w}_f}\right)_{\text{const. } w_o}$ | $(r+1)\,(3-m)\,y\alpha$ |
| $\left(\frac{\Delta p/\overline{p}}{\Delta w_o/\overline{w}_o}\right)_{\text{const. } r}$; $\left(\frac{\Delta p/\overline{p}}{\Delta w_f/\overline{w}_f}\right)_{\text{const. } r}$ | $(3-m)\,y\alpha$ |

The parameter $Q$ will be referred to as the "injection-velocity sensitivity" since its magnitude determines to what extent the response will be affected by the perturbation in injection velocity for a given value of time lag and interaction index.

The frequency response defined by the general transfer function for various values of $Q$ and $\bar{\tau}$ is presented in figures 3 and 4 at the end of this report. (The value of $n$ is kept constant at 0.5 in these figures.) The amplitudes (fig. 3) and the phase shifts (fig. 4) are given as functions of the dimensionless frequency of neutral oscillation $\beta$. This dimensionless frequency, of course, is equivalent to the dimensional angular frequency multiplied by the gas residence time. (In using the computations presented herein, it is well to note that the imposed frequency limit can be expressed approximately as $\beta \ll 1/\text{Mach number}$.) The range of values shown for the sensitivity parameter $Q$ is believed to be a realistic one. Consider, for example, a combustion process conforming to the approximate values previously discussed for the quantities $m$, $y$, and $\alpha$ (3/2, 1, and 2/3, respectively); the value of the sensitivity $Q$ would then be unity for the transfer functions $\left(\frac{\Delta p/\overline{p}}{\Delta w_o/\overline{w}_o}\right)_{\text{const. } r}$ and $\left(\frac{\Delta p/\overline{p}}{\Delta w_f/\overline{w}_f}\right)_{\text{const. } r}$ and even larger for the transfer function $(r+1)\left(\frac{\Delta p/\overline{p}}{\Delta w_f/\overline{w}_f}\right)_{\text{const. } w_o}$. All the transfer functions, of course, would yield the curves shown for the zero-sensitivity case $\frac{r+1}{r}\left(\frac{\Delta p/\overline{p}}{\Delta w_o/\overline{w}_o}\right)_{\text{const. } w_f}$ if the injection-velocity effect had been neglected in the time-lag concept. These curves, therefore, can be used as a basis of comparison for the more general time-lag concept.

From this information presented in figures 3 and 4, it can be concluded that the injection-velocity effect on the time lag is an important factor to consider when treating the dynamics of the combustion chamber. This is evident upon noting the strong dependence of the frequency response on the value of the injection-velocity sensitivity. At the higher values of the sensitivity parameter, both the amplitude and phase curves are considerably different than those for a sensitivity of zero. It should be noticed, too, that the difference becomes greater with increasing time lag.

### STABILITY CONSIDERATIONS

For an analysis of combustion instability, the chamber equation (eq. (18)) must be considered together with appropriate equations for the fuel and oxidizer feeding systems. An equation for propellant-feed systems that can be applied to either pump- or tank-fed rockets is presented in reference 11. This equation, with certain simplifying assumptions, takes into account the resistance, inductance, and capacitance of the feeding system. In stability evaluations of particular systems, in which these effects are specified by given constants, the equation can be used without difficulty. A general treatment, however,

becomes very involved when the complete equation is used.

Therefore, in order to show without undue complication the relative importance of the injection-velocity effect, a simple, tank-fed system with negligible capacitance and inductance is assumed for both propellants in the present treatment. Such a system represents the limiting case approached by tank-fed rockets with short lines. The simplified equations for the fuel and oxidizer feeding systems can be written as follows (both tanks have the same pressure):

$$\frac{\Delta w_f}{\overline{w}_f}=-K\frac{\Delta p}{\overline{p}} \tag{23}$$

$$\frac{\Delta w_o}{\overline{w}_o}=-K\frac{\Delta p}{\overline{p}} \tag{24}$$

where

$$K=\frac{\overline{p}}{2(P_{o,f}-\overline{p})}$$

The eliminant of equations (18), (23), and (24) yields the following characteristic equation:

$$1+s-n(1-e^{-\overline{\tau}s})+Ke^{-\overline{\tau}s}(1+Q\overline{\tau}s)=0 \tag{25}$$

where

$$Q=(3-m)y\alpha$$

The characteristic equation determines the boundary between stable and unstable oscillation when the real part of the operator $s$ is zero. The operator, therefore, is set equal to $i\beta$, where $\beta$ is the dimensionless frequency of neutral oscillation. By separating the real and imaginary parts of equation (25), two real equations are obtained:

$$\left.\begin{aligned} Q\overline{\tau}K\beta\sin\overline{\tau}\beta&=n-1-(n+K)\cos\overline{\tau}\beta\\ Q\overline{\tau}K\beta\cos\overline{\tau}\beta&=-\beta+(n+K)\sin\overline{\tau}\beta\end{aligned}\right\} \tag{26}$$

Equations (26) represent the stability boundary in parametric form. Because of the transcendental nature of these equations, a single equation of the stability boundary cannot be obtained. The parametric equations, however, can be expressed in more convenient form.

Upon squaring and adding equations (26), it can be ascertained that

$$(Q\overline{\tau}K\beta)^2=\beta^2+(n-1)^2+(n+K)^2-2(n+K)\frac{n-1+\beta\tan\overline{\tau}\beta}{\sqrt{1+\tan^2\overline{\tau}\beta}} \tag{27}$$

Another equation is apparent after dividing the first of equations (26) by the second:

$$\frac{n-1+\beta\tan\overline{\tau}\beta}{\sqrt{1+\tan^2\overline{\tau}\beta}}=n+K \tag{28}$$

Introducing equation (28) into equation (27) (and rearranging) gives the following equation for $\overline{\tau}$ in terms of $\beta$ and the system parameters:

$$\overline{\tau}=\frac{\pm\sqrt{\beta^2+(n-1)^2-(n+K)^2}}{QK\beta} \tag{29}$$

where the square root is negative if, and only if, the parameter $Q$ is negative. The second relation required between $\overline{\tau}$ and $\beta$ is given by equation (28), which can be put in the quadratic form

$$[(n+K)^2-\beta^2]\tan^2\overline{\tau}\beta-2(n-1)\beta\tan\overline{\tau}\beta+(n+K)^2-(n-1)^2=0 \tag{30}$$

From equation (30), it is found that

$$\tan\overline{\tau}\beta=-\frac{(n-1)\beta\pm(n+K)\sqrt{\beta^2+(n-1)^2-(n+K)^2}}{\beta^2-(n+K)^2} \tag{31}$$

where the square root again bears the sign of $Q$. Solving equation (31) for $\overline{\tau}$ gives the equation

$$\overline{\tau}=\frac{1}{\beta}\left[a\pi-\tan^{-1}\frac{(n-1)\beta+(n+K)\sqrt{\beta^2+(n-1)^2-(n+K)^2}}{\beta^2-(n+K)^2}\right] \tag{32}$$

where the principal value of the arctangent is used $\left(-\frac{\pi}{2}<\tan^{-1}<\frac{\pi}{2}\right)$ and $a$ is an integer. For the present purpose, consideration is limited to the fundamental oscillatory mode, that is, the mode corresponding to the smallest time lag satisfying equation (32); thus, the integer $a$ is given a value of unity. The stability boundary, therefore, is expressed by writing equations (29) and (32) in the following simultaneous form:

$$\left.\begin{aligned}\overline{\tau}&=\frac{\pm\sqrt{\beta^2+(n-1)^2-(n+K)^2}}{QK\beta}\\ \overline{\tau}&=\frac{1}{\beta}\left[\pi-\tan^{-1}\frac{(n-1)\beta\pm(n+K)\sqrt{\beta^2+(n-1)^2-(n+K)^2}}{\beta^2-(n+K)^2}\right]\end{aligned}\right\} \tag{33}$$

Equations (33) can be solved directly for two special cases. First, it is readily seen that, when the time lag is constant ($Q=0, n=0$), the solution is as follows:

$$\bar{\tau}=\frac{1}{\beta}(\pi-\tan^{-1}\beta) \tag{34}$$

where

$$\beta=\sqrt{K^2-1}$$

The second case is that of a time lag dependent on chamber pressure but independent of injection velocity ($Q=0$, $n\neq 0$). The following solution is then obtained:

$$\bar{\tau}=\frac{1}{\beta}\left(\pi-\tan^{-1}\frac{\beta}{1-n}\right) \tag{35}$$

where

$$\beta=\sqrt{(n+K)^2-(n-1)^2}$$

For the general case, equations (33) were solved numerically by iterative procedure with a high-speed digital computer. The stability boundaries obtained are presented in figure 5 at the end of this report. The critical values of the time lag $\bar{\tau}$, that is, the values giving neutral oscillation, are shown as functions of the injection-velocity sensitivity $Q$ for various values of feed system pressure drop $(P_{o,f}-\bar{p})/\bar{p}$. This pressure-drop parameter, of course, is equivalent to the quantity $1/2K$. Separate charts are given for different values of the interaction index $n$. The unstable domain associated with each stability boundary is represented by the region of the figure above the boundary. Curves of constant critical frequency $\beta$ (dashed lines) are also given in the charts.

The conclusion drawn from figure 5 is that the injection-velocity sensitivity cannot be neglected in the theory of low-frequency combustion instability. As shown in the figure, the critical time lag for a given interaction index and pressure drop is highly dependent on the magnitude of the injection-velocity sensitivity. The influence of the sensitivity parameter $Q$ is shown to be generally destabilizing; however, it is also apparent that small values of the parameter $Q$ can be stabilizing. Comparing the three parts of the figure shows that the destabilizing effect of the larger sensitivities is greater at the smaller values of interaction index.

This latter observation is more evident from figure 6, where, for a constant pressure drop,

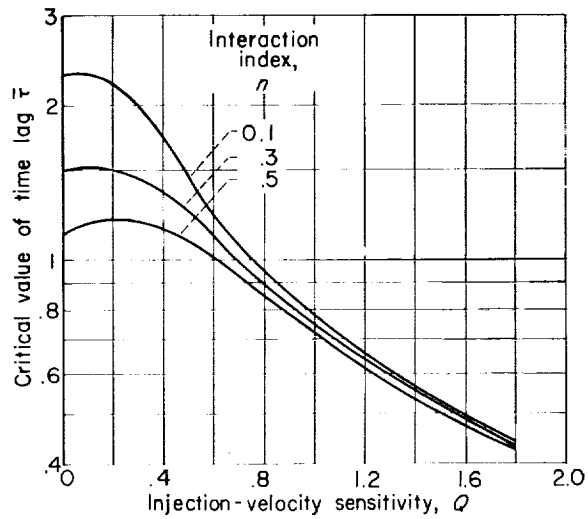


FIGURE 6. Effect of interaction index $n$ on stability boundary. Pressure drop $(P_{o,f}-\bar{p})/\bar{p}$, 0.4.

stability boundaries for different values of interaction index are shown together. This figure also shows the influence of the interaction index to be small at the higher values of the injection-velocity sensitivity.

In the final figure (fig. 7), the critical curves for an interaction index of 0.2 are given for

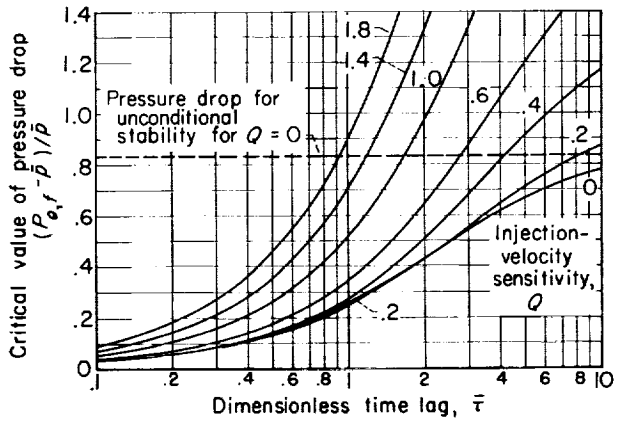


FIGURE 7.—Effect of injection-velocity sensitivity $Q$ on unconditional stability. Interaction index $n$, 0.2.

constant values of injection-velocity sensitivity with the pressure drop and time lag as ordinate and abscissa, respectively. With this low value of interaction index, there is, according to reference 11, a value of pressure drop large enough to make the system unconditionally stable, that is, stable

for all values of time lag. The criterion of reference 11 for unconditional stability can be written as

$$\frac{P_{o,f}-\bar{p}}{\bar{p}} \geq \frac{1}{2}\left(\frac{1}{1-2n}\right) \qquad \left(n<\frac{1}{2}\right)$$

For an interaction index of 0.2, the criterion yields a value of 0.83 for the pressure drop. This value is marked in figure 7 by the dashed line. Since the line is crossed by stability boundaries, it is evident that the criterion is not sufficient with the generalized time-lag concept. In fact, equation (29) indicates that unconditional stability does not exist for injection-velocity sensitivities other than zero. This can be shown upon writing the equation as follows:

$$\beta^2=\frac{(K+1)(2n+K-1)}{1-(\bar{Q\tau}K)^2} \tag{36}$$

Equation (36) determines the following two conditions having no real frequency of neutral oscillation:

(1) $K\leq 1-2n$ and $K<\left|\frac{1}{\bar{Q\tau}}\right| \qquad \left(n<\frac{1}{2}\right)$

(2) $K\geq 1-2n$ and $K>\left|\frac{1}{\bar{Q\tau}}\right|$

The first condition is the criterion for stability (the second for instability). In terms of pressure drop, it is expressed as follows:

$$\begin{cases} \dfrac{P_{o,f}-\bar{p}}{\bar{p}} \geq \dfrac{1}{2}\left(\dfrac{1}{1-2n}\right) & \left(n<\dfrac{1}{2}\right) \\ \dfrac{P_{o,f}-\bar{p}}{\bar{p}} > \dfrac{1}{2}\left|\bar{Q\tau}\right| \end{cases}$$

The criterion, although sufficient for stability, does involve the time lag; the stability, therefore, is not unconditional.

## CONCLUDING REMARKS

In conclusion, it is important to recall that the time-lag concept used herein was introduced because previous studies indicated a dependency of combustion time lag on injection velocity. The purpose of the present study was to show the importance of using this more general concept when treating chamber dynamics and stability.

The analyses made with the generalized concept of time lag have shown that chamber responses and system stability boundaries can be greatly affected in the low-frequency range by reasonable variations of the time lag with injection velocity. It can be concluded, therefore, that the injection-velocity effect on the time lag is an important factor to consider in the theory of chamber dynamics and combustion instability.

In view of this conclusion, it can be stated that information concerning the relation of drop size to injection velocity is essential for the accurate prediction of rocket dynamics and stability. Investigations, therefore, should be conducted to provide this information for the various injector types of interest.

LEWIS RESEARCH CENTER
NATIONAL AERONAUTICS AND SPACE ADMINISTRATION
CLEVELAND, OHIO, *April 24, 1959*

## REFERENCES

1. Ross, Chandler C., and Datner, Paul P.: Combustion Instability in Liquid-Propellant Rocket Motors—A Survey. Selected Combustion Problems Fundamentals and Aero. Applications, Butterworths Sci. Pub. (London), 1954, pp. 352–380.
2. Gunder, D. F., and Friant, D. R.: Stability of Flow in a Rocket Motor. Jour. Appl. Mech., vol. 17, no. 3, Sept. 1950, pp. 327–333.
3. Yachter, M., and Waldinger, H. V.: Dynamic Analysis of a Rocket Motor. Rep. SPD–241, Spec. Proj. Dept., M. W. Kellogg Co., Oct. 1, 1949. (See also Jour. Appl. Mech., vol. 18, no. 1, 1951, pp. 114–116.)
4. Summerfield, Martin: A Theory of Unstable Combustion in Liquid Propellant Rocket Systems. Jour. Am. Rocket Soc., vol. 21, no. 5, Sept. 1951, pp. 108–114.
5. Lee, Y. C., Gore, M. R., and Ross, C. C.: Stability and Control of Liquid Propellant Rocket System. Jour. Am. Rocket Soc., vol. 23, no. 2, Mar.–Apr. 1953, pp. 75–81.
6. Crocco, L.: Aspects of Combustion Stability in Liquid Propellant Rocket Motors. I Fundamental Low Frequency Instability with Monopropellants. Jour. Am. Rocket Soc., vol. 21, no. 6, Nov. 1951, pp. 163–178.
7. Crocco, L.: Aspects of Combustion Stability in Liquid Propellant Rocket Motors. II—Low Frequency Instability with Bipropellants. High Frequency Instability. Jour. Am. Rocket Soc., vol. 22, no. 1, Jan.–Feb. 1952, pp. 7–16.
8. Tsien, H. S.: Servo-Stabilization of Combustion in Rocket Motors. Jour. Am. Rocket Soc., vol. 22, no. 5, Sept.–Oct. 1952, pp. 256–262; 268.
9. Marble, F. E., and Cox, D. W., Jr.: Servo-Stabilization of Low-Frequency Oscillations in a Liquid Bipropellant Rocket Motor. Jour. Am. Rocket Soc., vol. 23, no. 2, Mar.–Apr. 1953, pp. 63–74; 81.
10. Crocco, L., Grey, J., and Matthews, G. B.: Preliminary Measurements of the Combustion Time Lag in a Monopropellant Rocket Motor. Fifth Symposium

(International) on Combustion, Reinhold Pub. Co., 1955, p. 164.

11. Crocco, Luigi, and Cheng, Sin-I: Theory of Combustion Instability in Liquid Propellant Rocket Motors. AGARDograph No. 8, Butterworths Sci. Pub. (London), 1956.
12. Shafer, M. R., and Bovey, H. L.: Applications of Dimensional Analysis to Spray-Nozzle Performance Data. Jour. Res. Nat. Bur. Standards, vol. 52, no. 3, Mar. 1954, pp. 141–147.
13. Ingebo, Robert D.: Drop-Size Distributions for Impinging-Jet Breakup in Airstreams Simulating the Velocity Conditions in Rocket Combustors. NACA TN 4222, 1958.
14. Priem, Richard J.: Propellant Vaporization as a Criterion for Rocket-Engine Design; Calculations Using Various Log-Probability Distributions of Heptane Drops. NACA TN 4098, 1957.
15. Penner, S. S., and Fuhs, A. E.: On Generalized Scaling Procedures for Liquid-Fuel Rocket Engines. Combustion and Flame, vol. 1, no. 2, June 1957, pp. 229–240.
16. Crocco, L., Grey, J., and Harrje, D. T.: On the Importance of the Sensitive Time Lag in Longitudinal High-Frequency Rocket Combustion Instability. Jet. Prop., vol. 28, no. 12, Dec. 1958, p. 841.
17. Spalding, D. B.: Combustion of a Single Droplet and of a Fuel Spray. AGARD Selected Combustion Problems—Fundamentals and Aero. Applications, Butterworths Sci. Pub. (London), 1954, pp. 340–351.
18. Frössling, Nils: Über die Verdunstung fallender Tropfen. Gerl. Beitr. Geophys., Bd. 52, Heft 1/2, 1938, pp. 170–216.
19. Priem, Richard J.: Propellant Vaporization as a Criterion for Rocket-Engine Design; Calculations of Chamber Length to Vaporize Various Propellants. NACA TN 3883, 1958.
20. Cheng, Sin-I: Low-Frequency Combustion Stability of Liquid Rocket Motor with Different Nozzles. Jour. Am. Rocket Soc., vol. 25, no. 4, Apr. 1955, pp. 163–167.
21. Tsien, H. S.: Transfer Functions of Rocket Nozzles. Jour. Am. Rocket Soc., vol. 22, May–June 1952, pp. 139–143; 162.
22. Crocco, L.: Supercritical Gaseous Discharge with High Frequency Oscillations. L'Aerotecnica, vol. 33, no. 1, Feb. 1953, pp. 46–53.

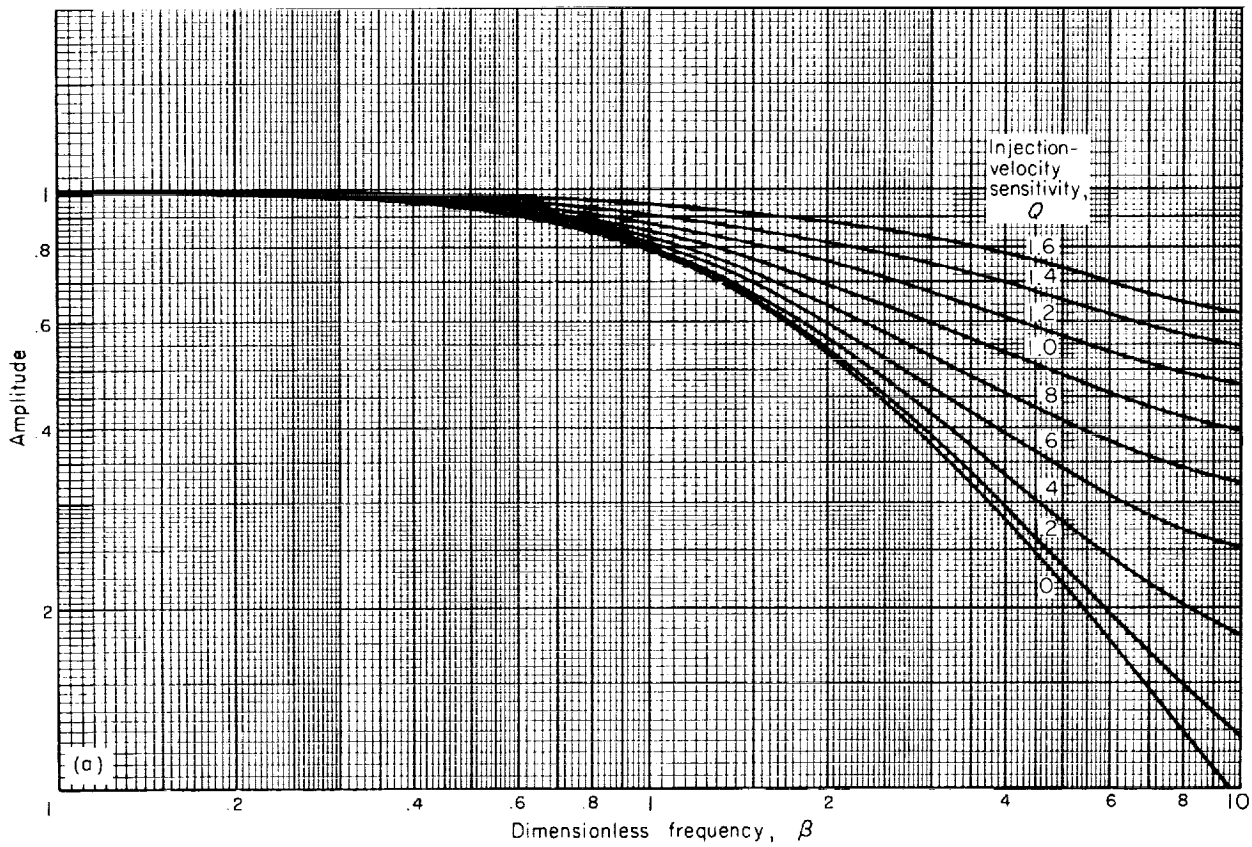


(a) Dimensionless time lag $\bar{\tau}$, 0.4.

FIGURE 3.—Amplitude of frequency response for general form of normalized transfer functions. Interaction index $n$, 0.5.

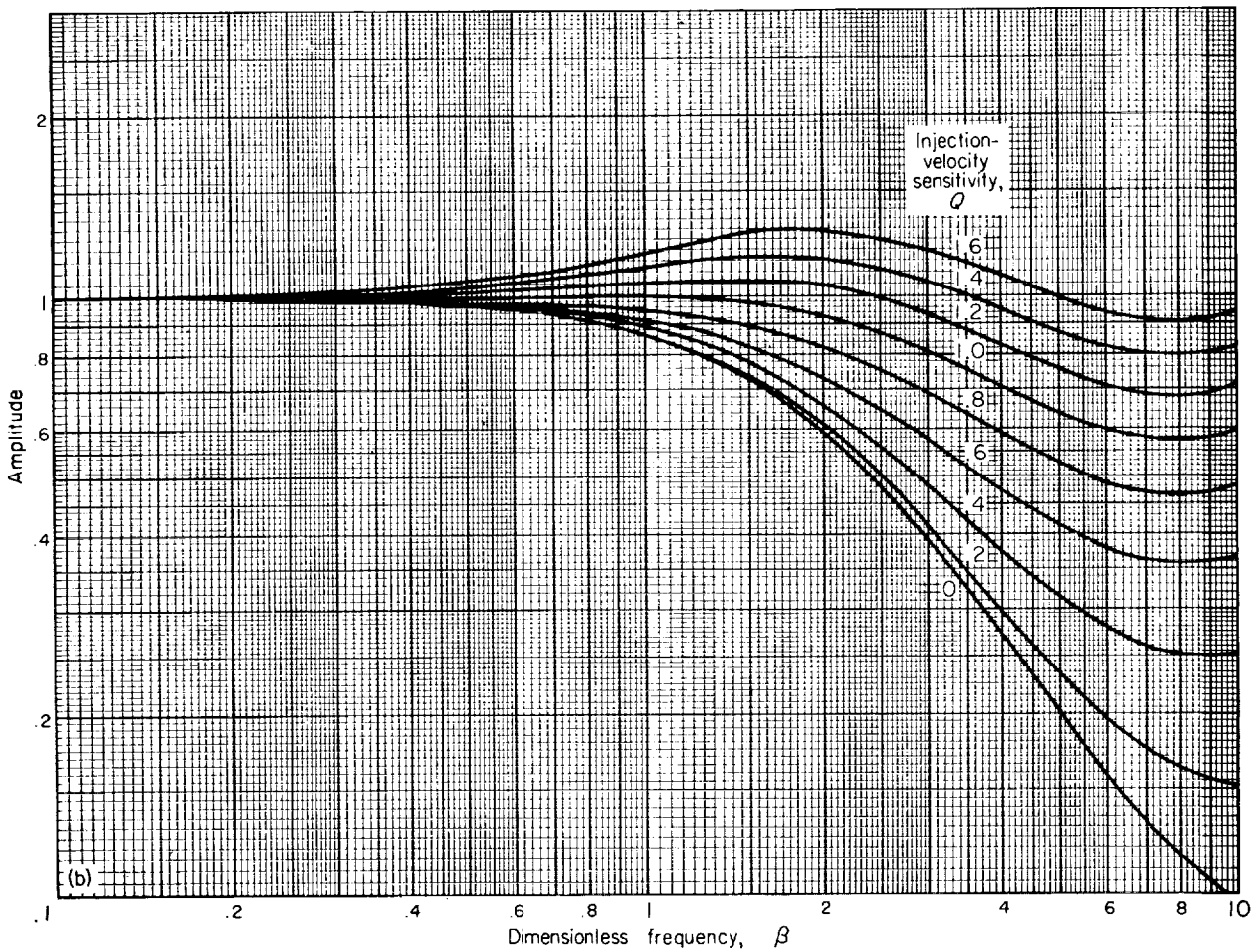


(b) Dimensionless time lag $\bar{\tau}$, 0.6.

FIGURE 3. Continued. Amplitude of frequency response for general form of normalized transfer functions. Interaction index $n$, 0.5.

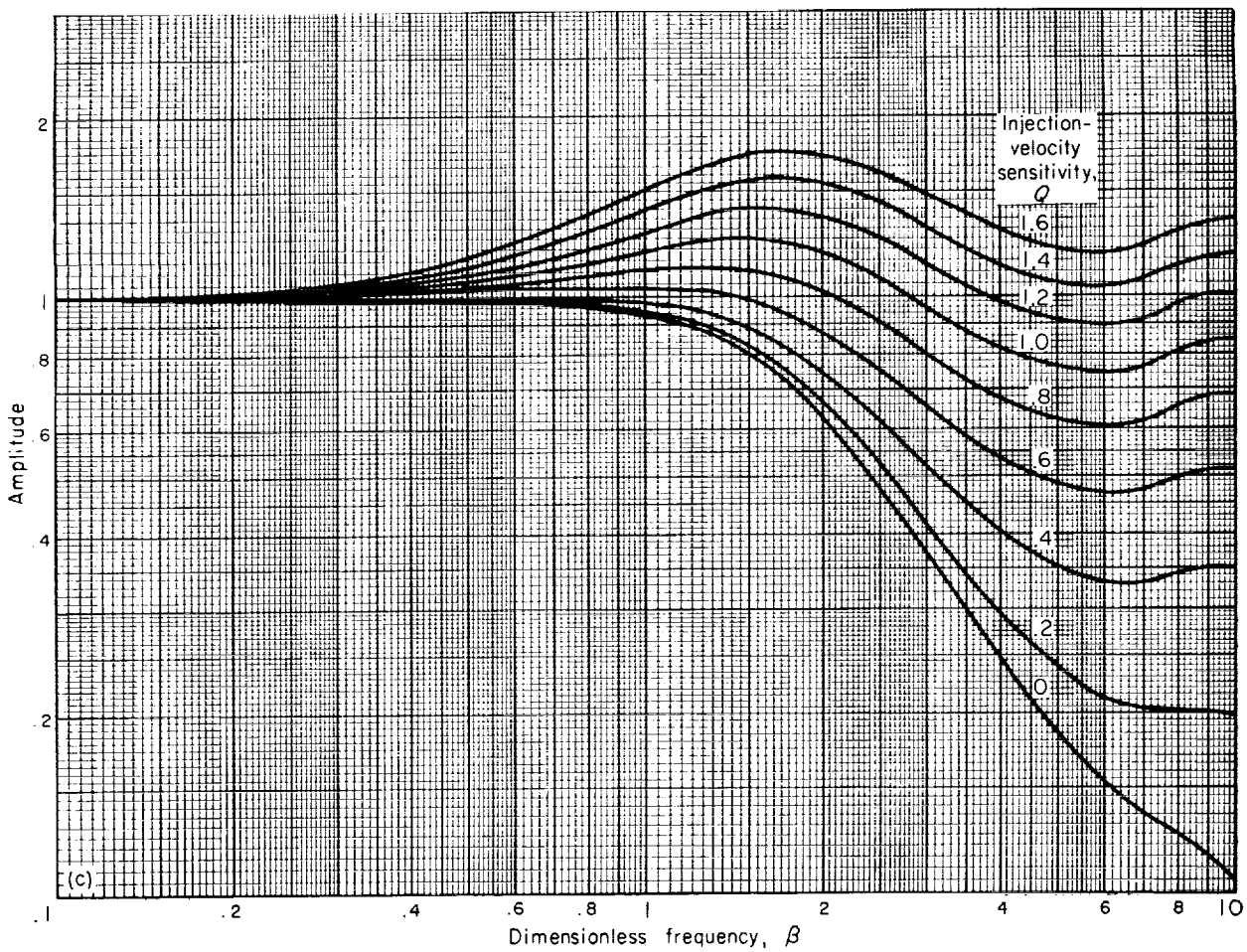


(c) Dimensionless time lag $\bar{\tau}$, 0.8.

FIGURE 3.—Continued. Amplitude of frequency response for general form of normalized transfer functions. Interaction index $n$, 0.5.

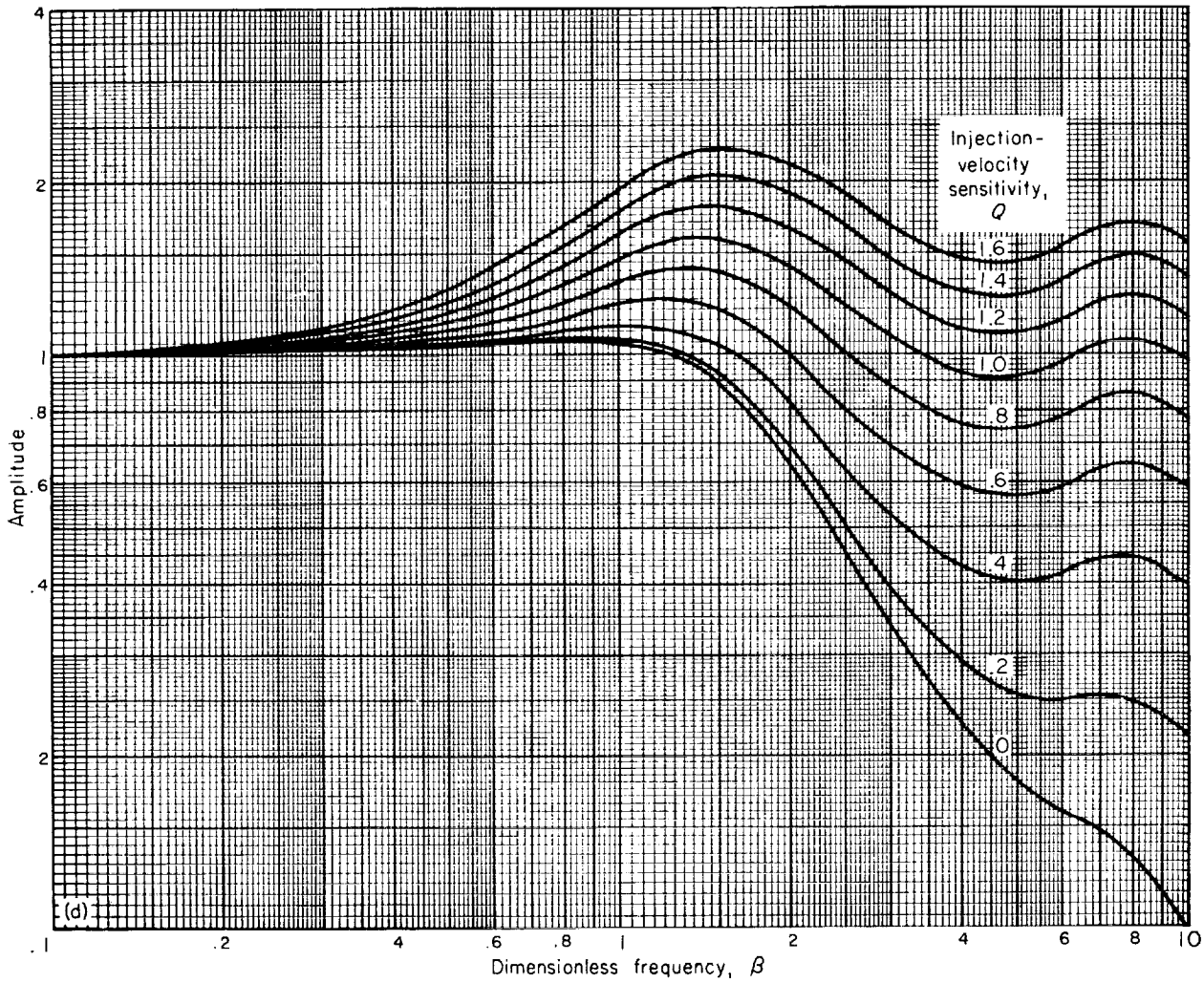


(d) Dimensionless time lag $\bar{\tau}$, 1.0.

FIGURE 3.—Continued. Amplitude of frequency response for general form of normalized transfer functions. Interaction index $n$, 0.5.

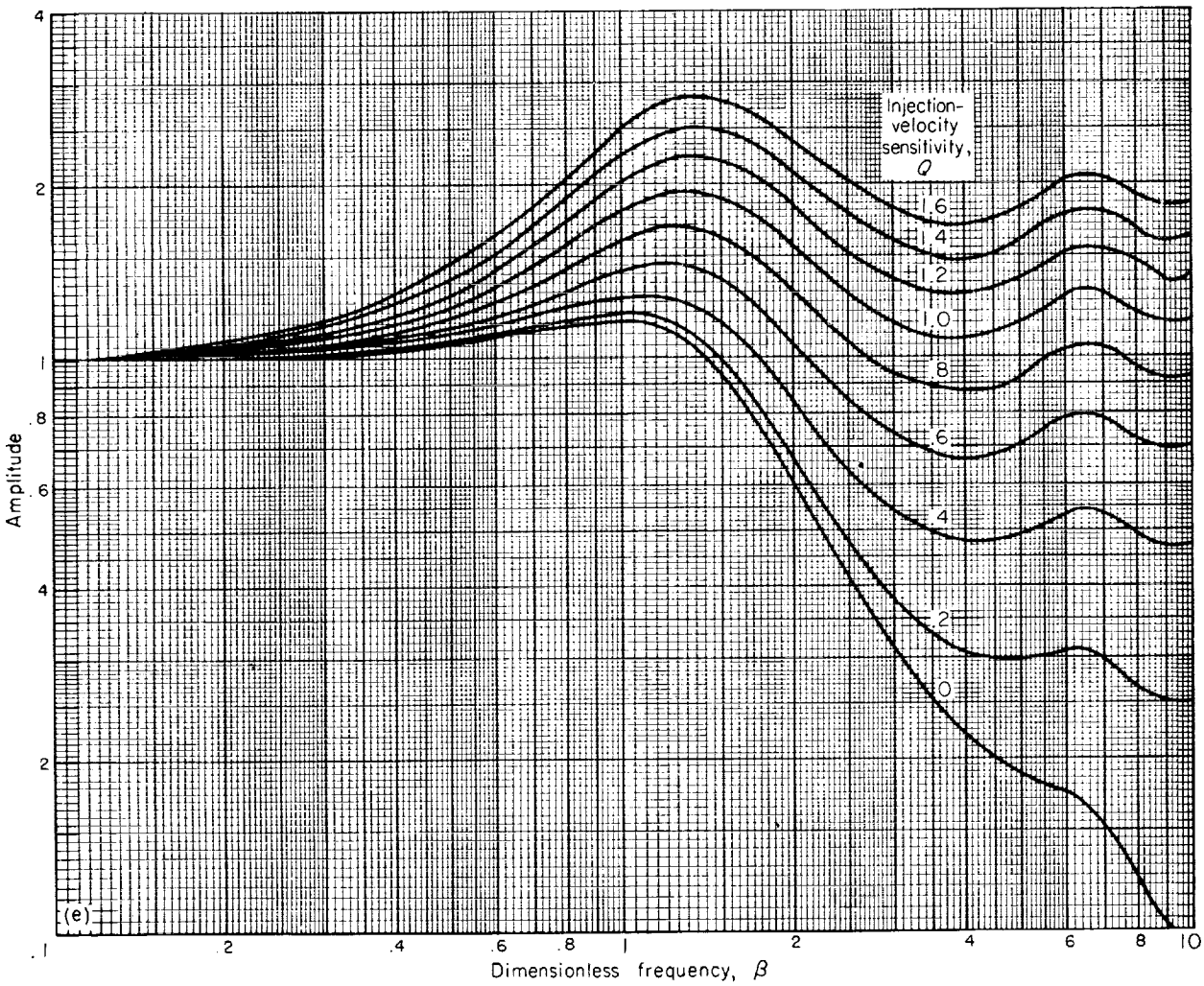


(c) Dimensionless time lag $\bar{\tau}$, 1.2.

FIGURE 3.- Continued. Amplitude of frequency response for general form of normalized transfer functions. Interaction index $n$, 0.5.

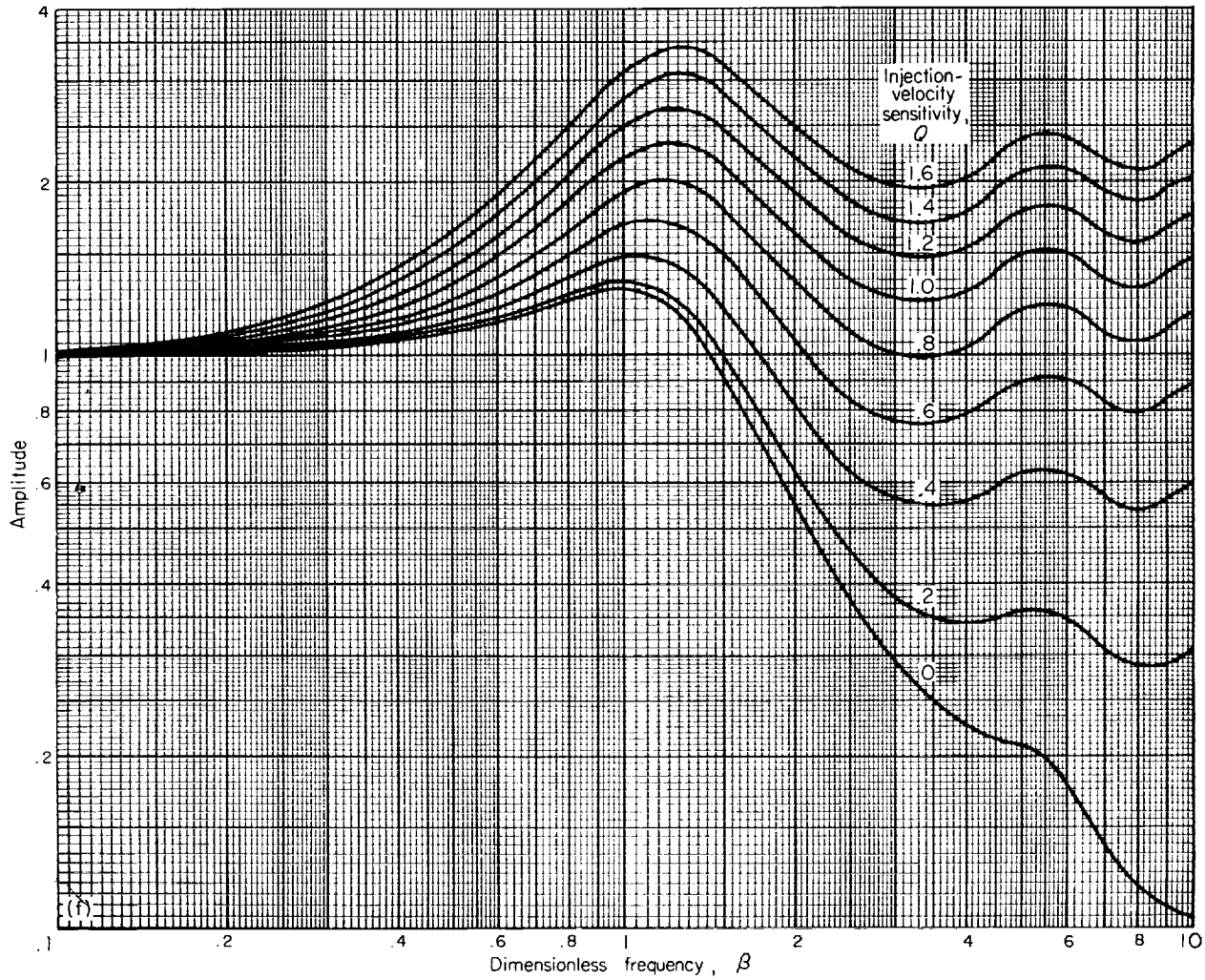


(f) Dimensionless time lag $\bar{\tau}$, 1.4.

FIGURE 3.– Concluded. Amplitude of frequency response for general form of normalized transfer functions. Interaction index $n$, 0.5.

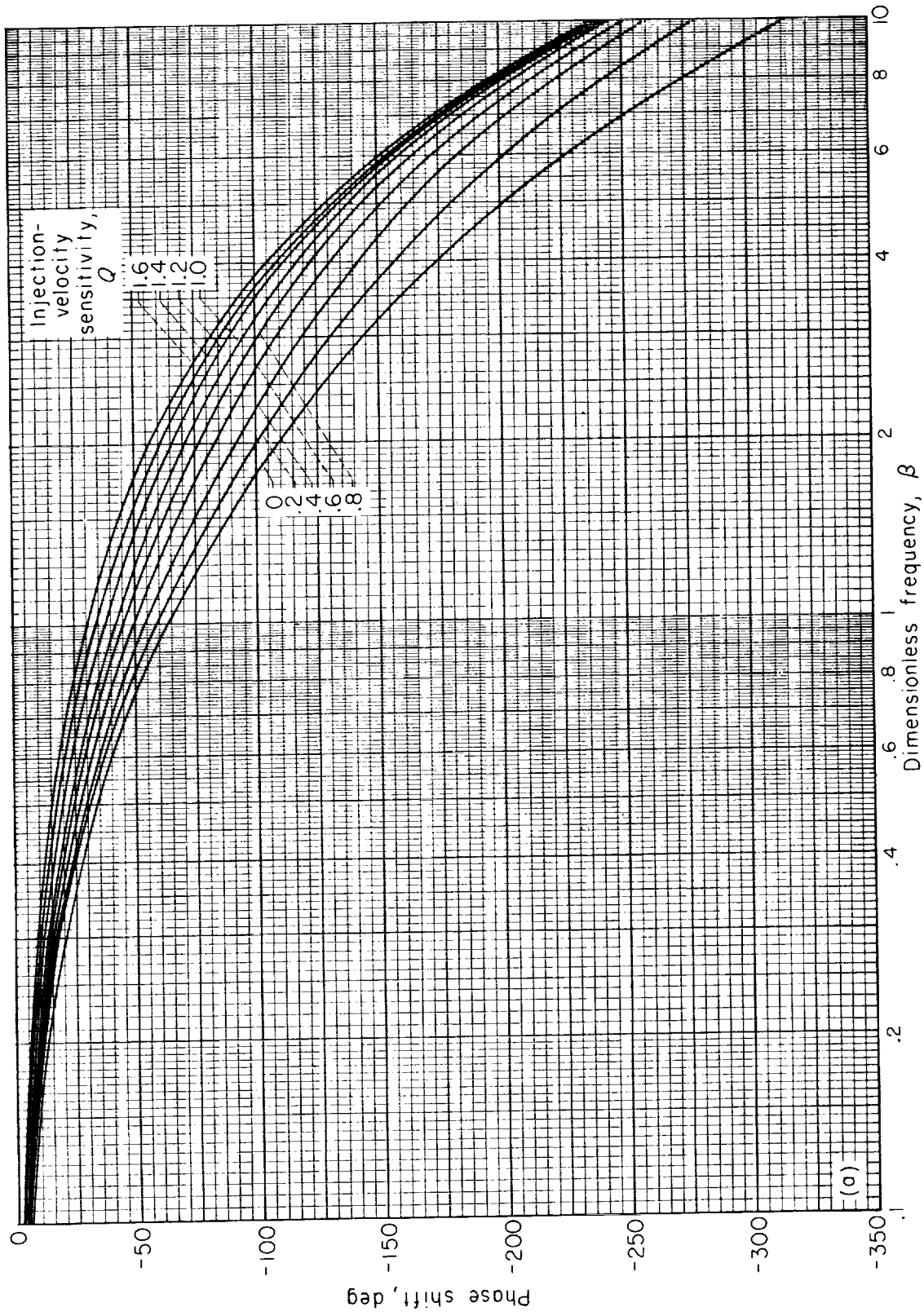


(a) Dimensionless time lag $\bar{\tau}$, 0.4.

FIGURE 4.—Phase shift of frequency response for general form of normalized transfer functions. Interaction index $n$, 0.5.

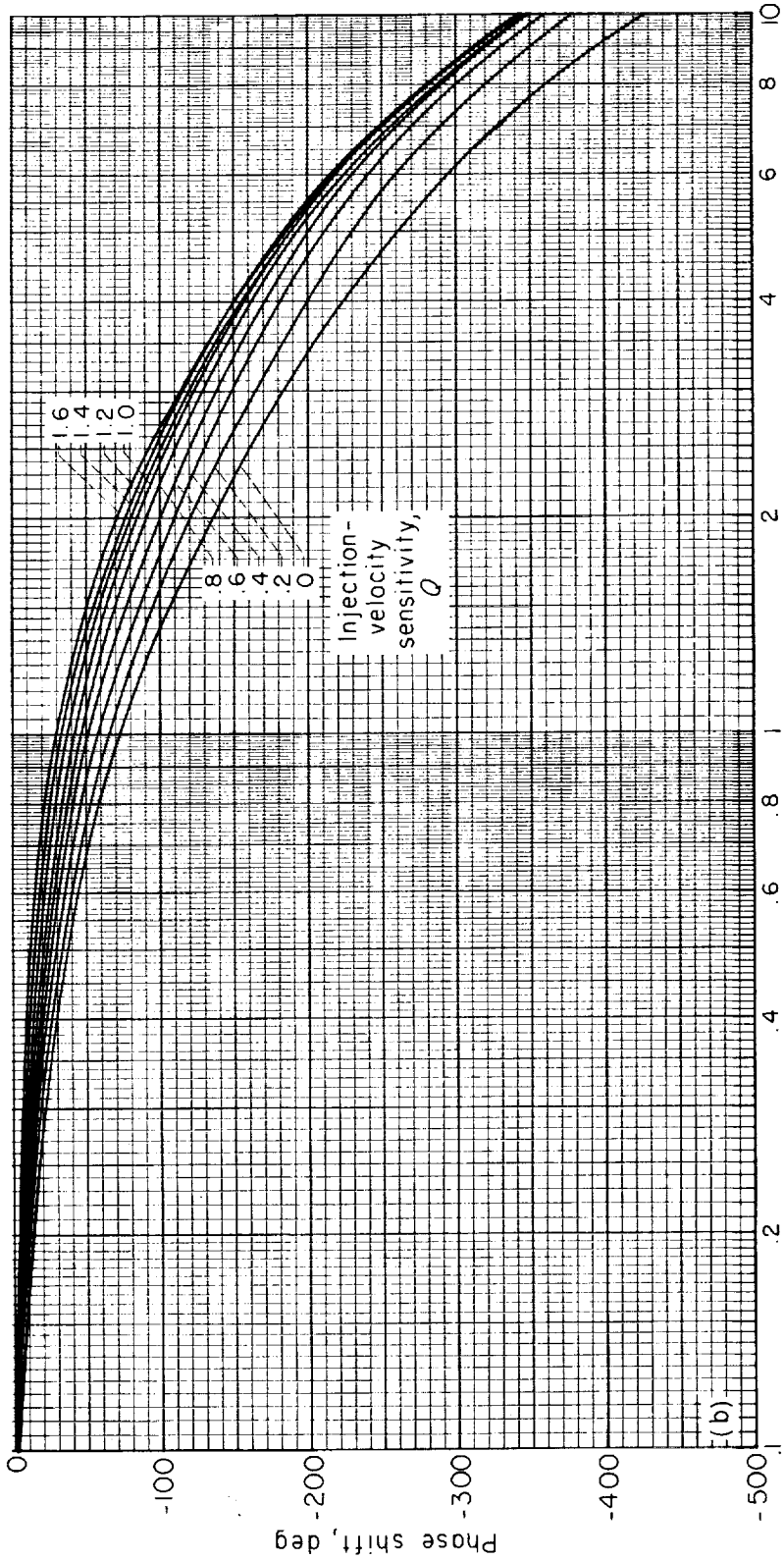


(b) Dimensionless time lag $\bar{\tau}$, 0.6.

FIGURE 4.—Continued. Phase shift of frequency response for general form of normalized transfer functions. Interaction index $n$, 0.5.

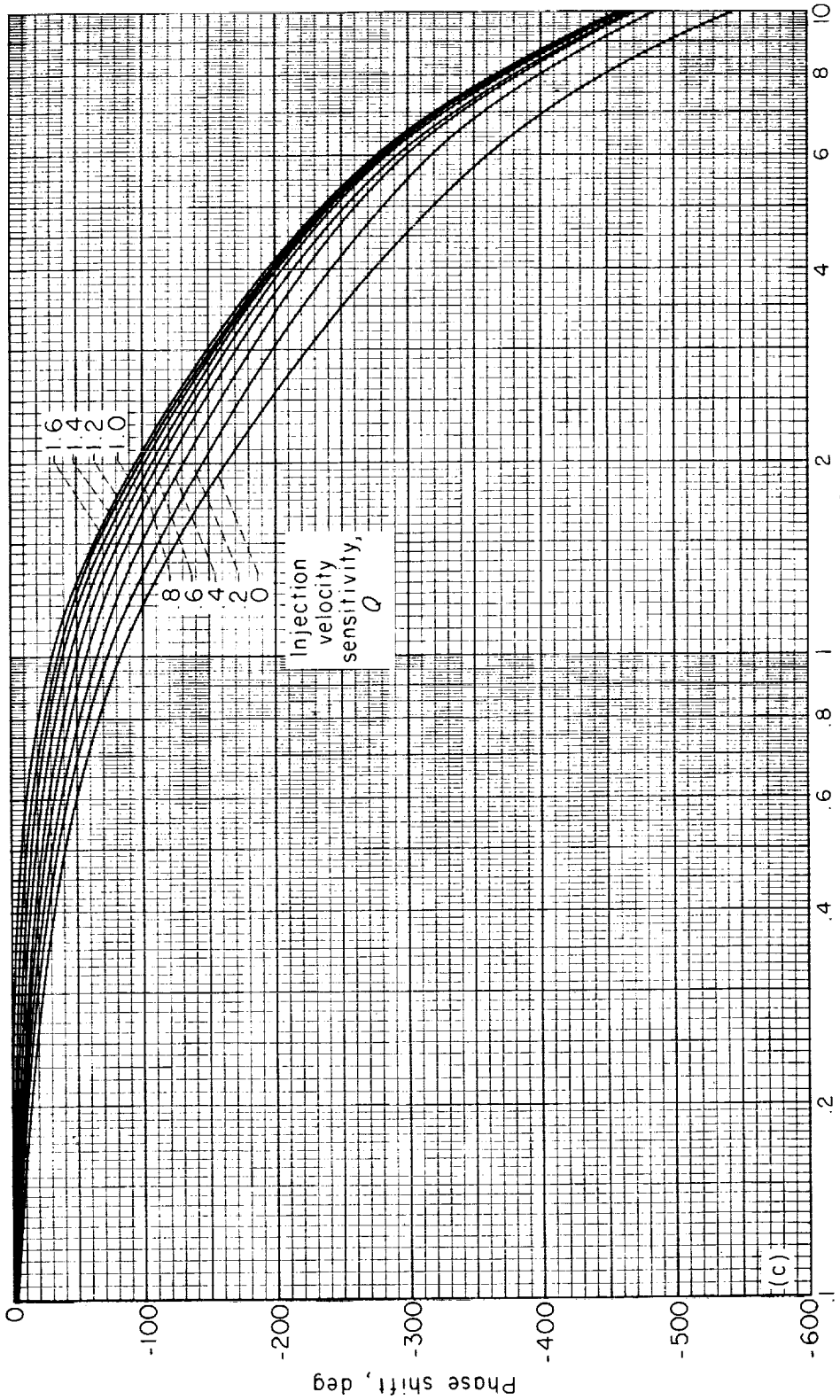


(c) Dimensionless time lag $\bar{\tau}$, 0.8.

FIGURE 4.—Continued. Phase shift of frequency response for general form of normalized transfer functions. Interaction index $n$, 0.5.

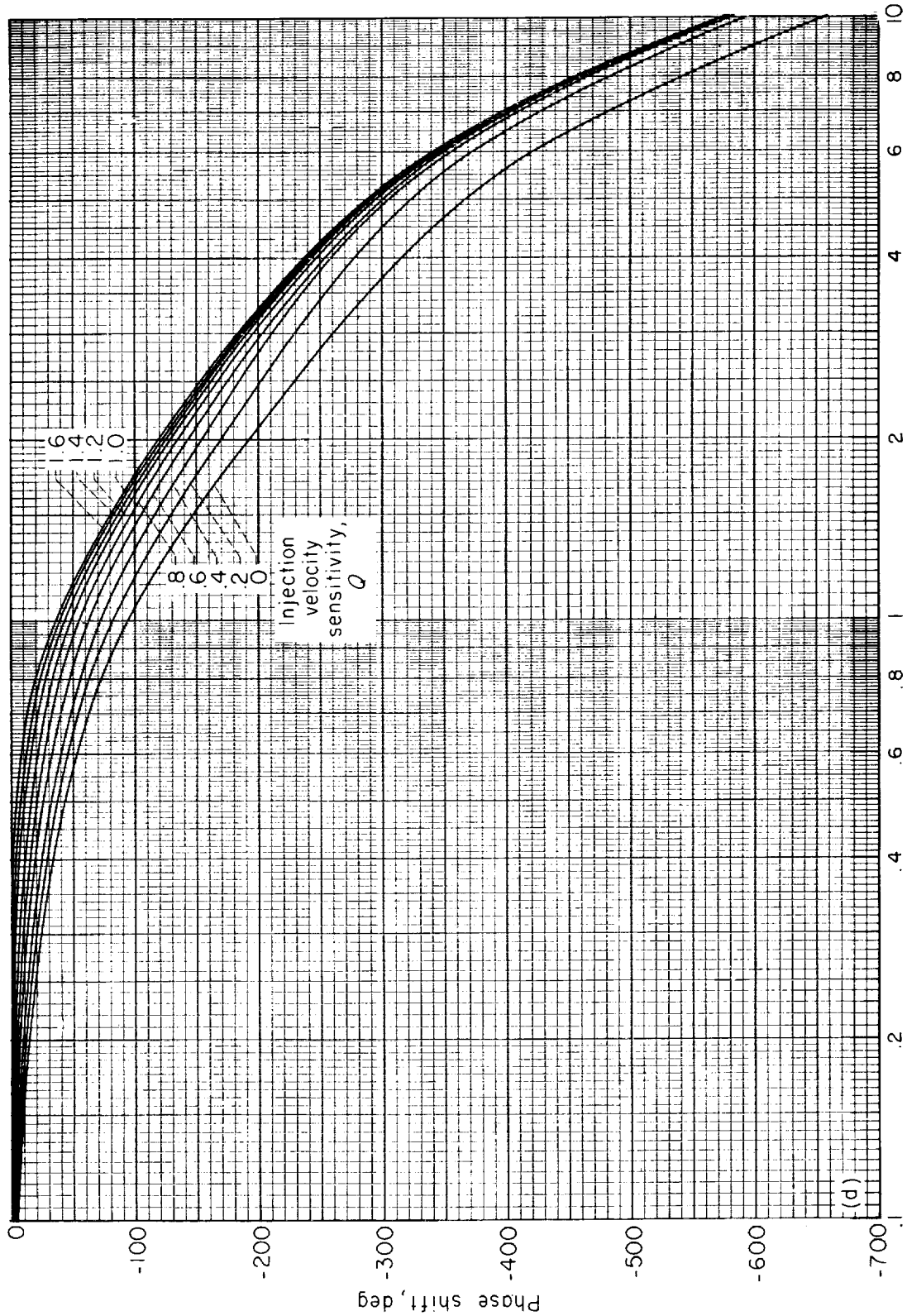


(d) Dimensionless time lag $\bar{\tau}$, 1.0.

FIGURE 4.—Continued. Phase shift of frequency response for general form of normalized transfer functions. Interaction index $n$, 0.5.

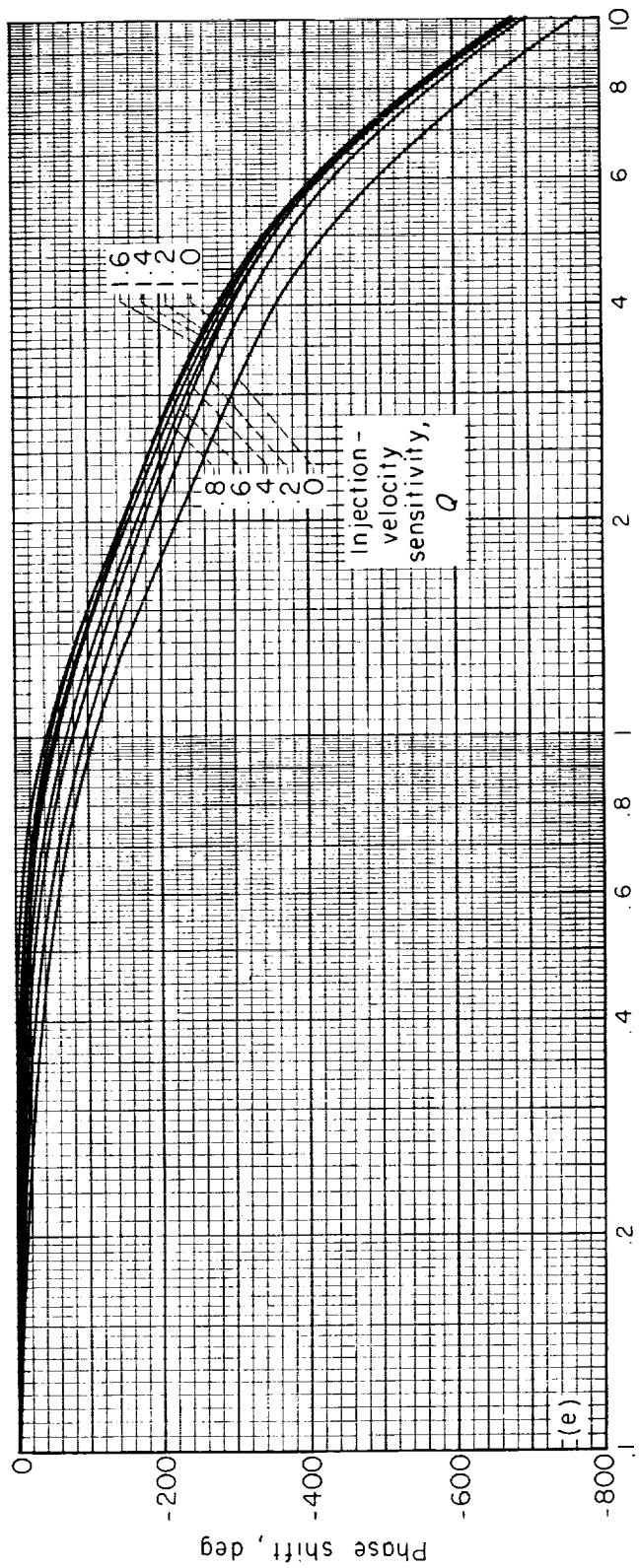


(e) Dimensionless time lag $\bar{\tau}$, 1.2.

FIGURE 4.—Continued. Phase shift of frequency response for general form of normalized transfer functions. Interaction index $n$, 0.5.

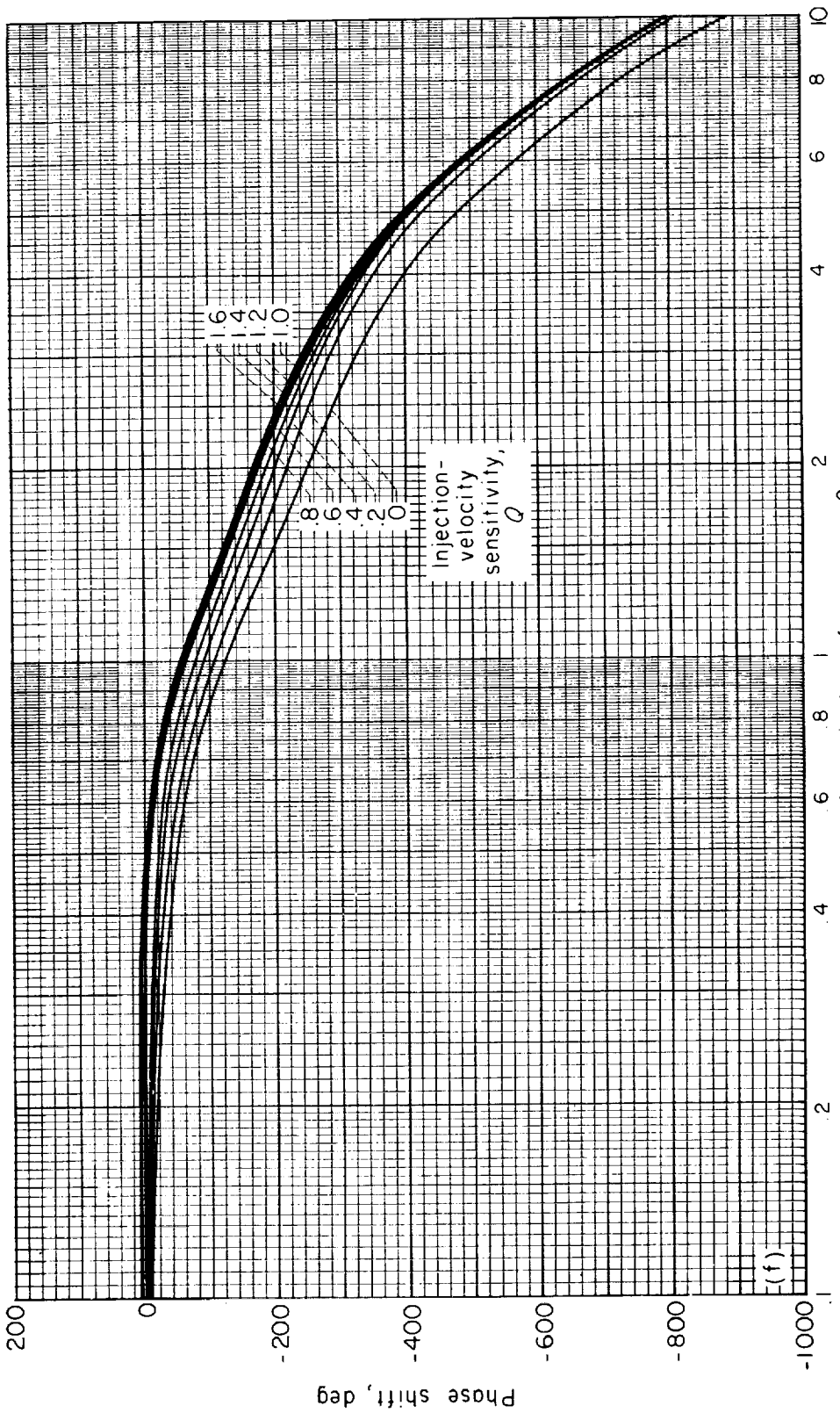


(f) Dimensionless time lag $\bar{\tau}$, 1.4.

FIGURE 4.—Concluded. Phase shift of frequency response for general form of normalized transfer functions. Interaction index $n$, 0.5.

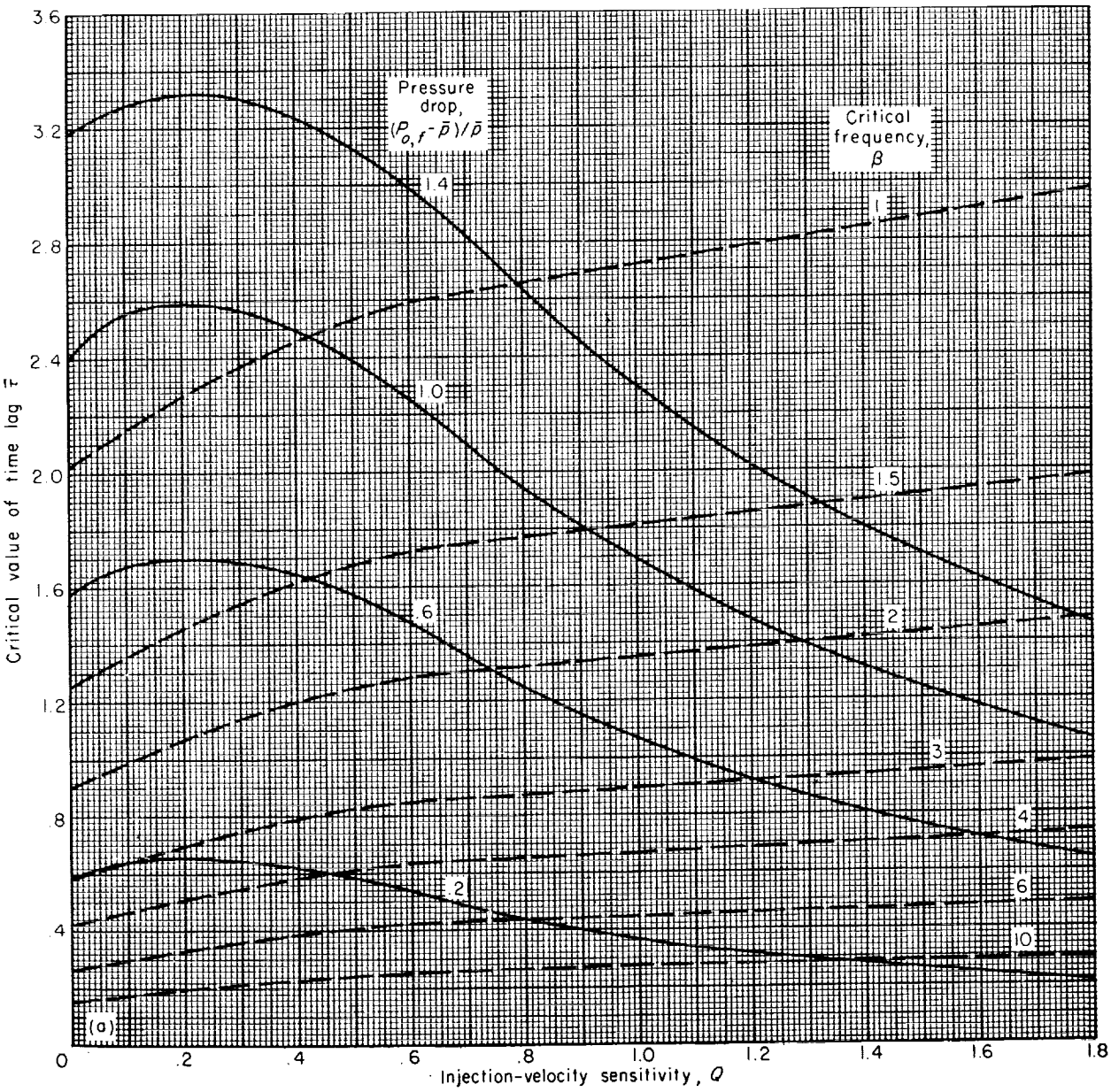


(a) Interaction index $n$, 0.5.

FIGURE 5.—Stability boundaries of tank-fed rocket with negligible feeding system inductance and capacitance.

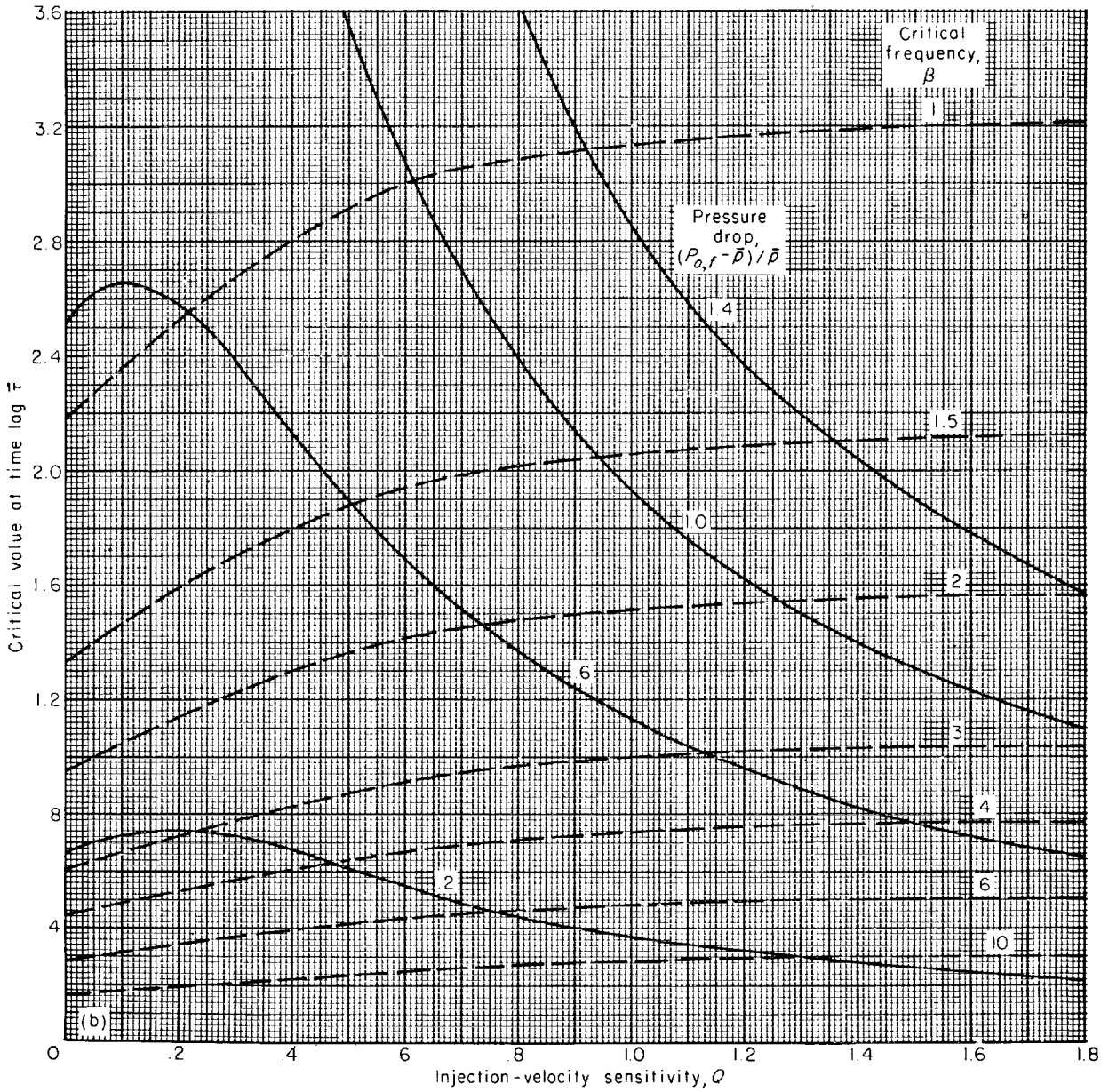


(b) Interaction index $n$, 0.3.

FIGURE 5.—Continued. Stability boundaries of tank-fed rocket with negligible feeding system inductance and capacitance.

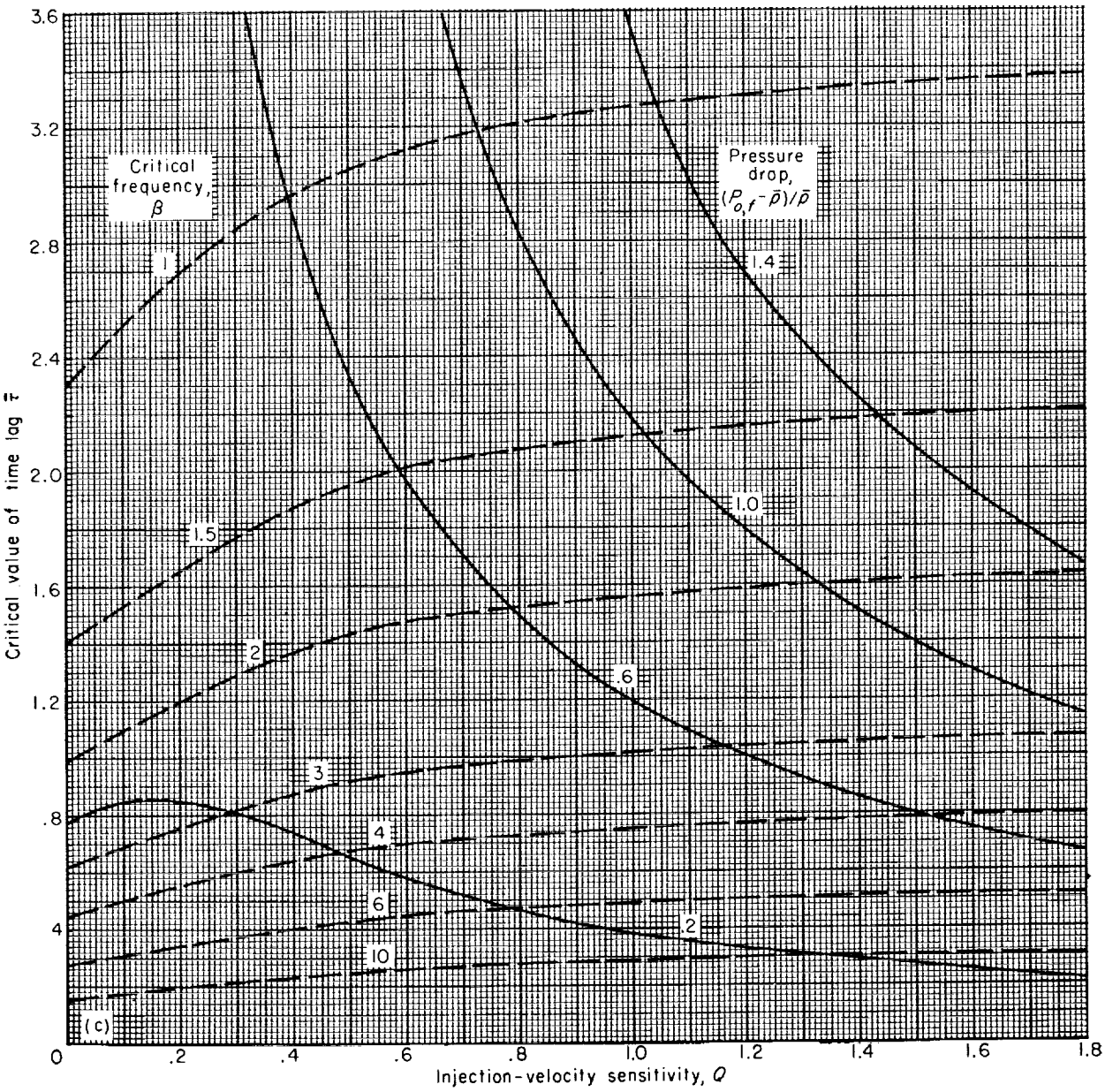


(c) Interaction index $n$, 0.1.

FIGURE 5.—Concluded. Stability boundaries of tank-fed rocket with negligible feeding system inductance and capacitance.

U.S. GOVERNMENT PRINTING OFFICE: 1960